Journal of Marine Systems 219 (2021) 103557

Contents lists available at ScienceDirect

Journal of Marine Systems

journal homepage: www.elsevier.com/locate/jmarsys

Environmental evolution of the Basque Coast Geopark estuaries (southern Bay of Biscay) during the last 10,000 years

Alejandro Cearreta [a,b,*], María Jesús Irabien [a], José E. Gómez Arozamena [c], Naima El bani Altuna [d], Aintzane Goffard [a], Ane García-Artola [a]

[a] Departamento de Geología, Facultad de Ciencia y Tecnología, Universidad del País Vasco UPV/EHU, Apartado 644, 48080 Bilbao, Spain
[b] Basque Centre for Climate Change (BC3), Edificio Sede 1, UPV/EHU Zientzia Parkea, Bº Sarriena s/n, 48940 Leioa, Spain
[c] Departamento de Ciencias Médicas y Quirúrgicas, Facultad de Medicina, Universidad de Cantabria, Avenida Herrera Oria s/n, 39011 Santander, Spain
[d] CAGE-Centre for Arctic Gas Hydrate, Environment and Climate, Department of Geosciences, UiT The Arctic University of Norway, Framstredet 10, 9019 Tromsø, Norway

ARTICLE INFO

Keywords:
Sedimentary record
Foraminifera
Trace metals
Radioisotopes
Holocene
Anthropocene

ABSTRACT

In order to reconstruct the environmental evolution of the Deba and Urola estuaries located in the Basque Coast Geopark at millennial, centennial and decadal timescales, four long boreholes, three short cores and twelve surface samples were studied. Multiproxy analysis (foraminifera, trace metals and radioisotopes) shows the temporal transformation of these estuaries in response to regional driving forces such as fresh-water discharge, relative sea-level (RSL) variation and the more recent impact of industrial development. At millennial and centennial timescales, the Deba estuary transformed from a tide-dominated to a river-dominated estuary at about 8000 yr cal BP following the decrease in RSL rise rate. This decrease also led to a reduction in both salinity and marine influence in the nearby tide-dominated Urola estuary. At decadal timescale, human disturbance on foraminiferal populations was found to be lower in the Deba estuary despite its higher level of contaminants in sediments. This was due to the greater impact of fresh-water discharge. In the Urola estuary, dredging operations altered severely the foraminiferal biota.

1. Introduction

Estuarine environments are located at the interface between marine and terrestrial realms. Consequently, they are characterised by strong environmental gradients and high variability of their physico-chemical parameters (e.g., salinity and grain-size). Natural processes (such as sea-level rise, fresh-water supply, sediment availability and deposition rates) have represented the main environmental drivers of estuarine infilling during the Holocene Epoch (Perillo, 1995). Additionally, these naturally stressed environments have been subjected to a great variety of superimposed human perturbations (e.g., land reclamation, sewage and industrial waste disposal, biotic replacement and dredgings) during recent centuries on a worldwide basis (Lotze et al., 2006).

Estuaries appear as one of the most threatened ecosystems and a notable growth in research has been devoted to natural and anthropogenic fingerprints left in their geological record (Sun et al., 2012). These coastal ecosystems are of paramount importance because they provide more goods and services than many other biomes for the same unit area (Costanza et al., 1997). At present, there are numerous studies that monitor the ecological and chemical evolution with time in many estuaries of the world (Borja et al., 2016). Among the most abundant and ubiquitous shelled organisms in marine environments, foraminifera are considered useful past and present indicators in aquatic ecosystems worldwide because their species react in a rapid and sensitive way to environmental changes and they preserve in sediments due to the mineralised nature of their tests. If their modern ecology is known, the composition of fossil assemblages can be used for palaeoenvironmental reconstructions (Debenay et al., 2000). Existing literature shows that benthic foraminifera are widely used to study both present and past environmental conditions in many coastal ecosystems around the world (Cheng et al., 2012; Takata et al., 2014).

Located in the southeastern Bay of Biscay, the Basque coast has 246 km of length and is dominated by rocky vertical cliffs interrupted by 12 small estuaries with sandy beaches at their mouths. It represents only

* Corresponding author at: Departamento de Geología, Facultad de Ciencia y Tecnología, Universidad del País Vasco UPV/EHU, Apartado 644, 48080 Bilbao, Spain.
E-mail address: alejandro.cearreta@ehu.eus (A. Cearreta).

https://doi.org/10.1016/j.jmarsys.2021.103557
Received 29 September 2020; Received in revised form 22 February 2021; Accepted 13 April 2021
Available online 21 April 2021

12% of the total surface of the Basque Country, but it supports 60% of the total population and 33% of the industrial activities, both mainly concentrated around the lower estuarine areas (Cearreta et al., 2004). Human settlements and activities exert great pressure on these coastal environments. Such anthropogenic pressures over the estuaries have produced dramatic changes in their original physical, chemical and biological features during the last two centuries: around half of their original total surface has been lost by land reclamation (Rivas and Cendrero, 1992) and, additionally, they have received untreated urban and industrial wastewater discharges for a long time (Cearreta et al., 2004). Since the mid-20th century, local human impact has been considered as the major threat to the Basque coastal habitats compared with a more limited evidence of sea-level-rise-derived changes (Chust et al., 2009).

Estuaries are sedimentary systems that store critical geological information to reconstruct past environmental conditions on the coastal area during the last 10,000 years, as their sediments contain a wide variety of geological signatures adequate to perform a reliable environmental reconstruction through time. Multidisciplinary studies of their sedimentary record have been extensively used to examine the recent transformation and modern environmental conditions of estuarine areas (Baptista Neto et al., 2017; Ruiz-Fernández et al., 2016; Sreenivasulu et al., 2017). As sediments preserve a valuable fingerprint of natural events and human impacts, estuarine records provide useful information for investigating natural evolution and contamination histories, and for sustainable management of these coastal areas (Irabien et al., 2018). In order to analyse their natural and anthropogenic environmental transformations in response to postglacial variations in sea level and recent human activities, different sedimentary records have been collected from the Deba and Urola estuaries (Basque Coast Geopark). These estuaries share a similar history of natural transformation following Holocene deglaciation and sea-level rise as well as anthropogenic impact since the Industrial Revolution with other estuaries around the world. This work addresses a multidisciplinary approach including sedimentological, micropalaeontological and geochemical proxy data of 4 long boreholes, 3 short cores and 12 surface samples in order to put these sedimentary records into a multi-century perspective and also to perform a comparison of environmental conditions between these two intertidal settings at different temporal scales (millennial, centennial and decadal).

2. Study area

The Basque Coast Geopark (Fig. 1) was declared by UNESCO in 2010. It is located on the southeasternmost area of the Bay of Biscay, with a total extension of 90 km^2 and a 13 km-coastal front made of a near-continuous outcrop of lower Cretaceous to lower Eocene marine turbidite rocks (Baceta et al., 2010). It spans 60 million years of the Earth's history (from 110 to 50 Ma), and contains four major chronostratigraphic boundaries and two global boundary stratotype section and points (Selandian and Thanetian ages of the Paleocene Epoch). Intercalated with these vertical cliffs and their extensive wave-cut platform exposed at low tide, the small estuaries of Deba and Urola represent its only brackish environments, under semidiurnal and mesotidal conditions (<1 m in neap tides and 4.5 m during spring tides).

The Deba river valley contains abundant archaeological remains that suggest a continuous human presence since the Upper Palaeolithic (Peñalver et al., 2017). The Deba village, located at the estuary mouth (Fig. 1), was founded in 1343 and during the 14th to 16th centuries its port carried out a high comercial activity despite the presence of a well-developed sandy bar at the entrance of the estuary (Aldabaldetrecu, 1993). Reinforcement of the lower estuary and elimination of the bar

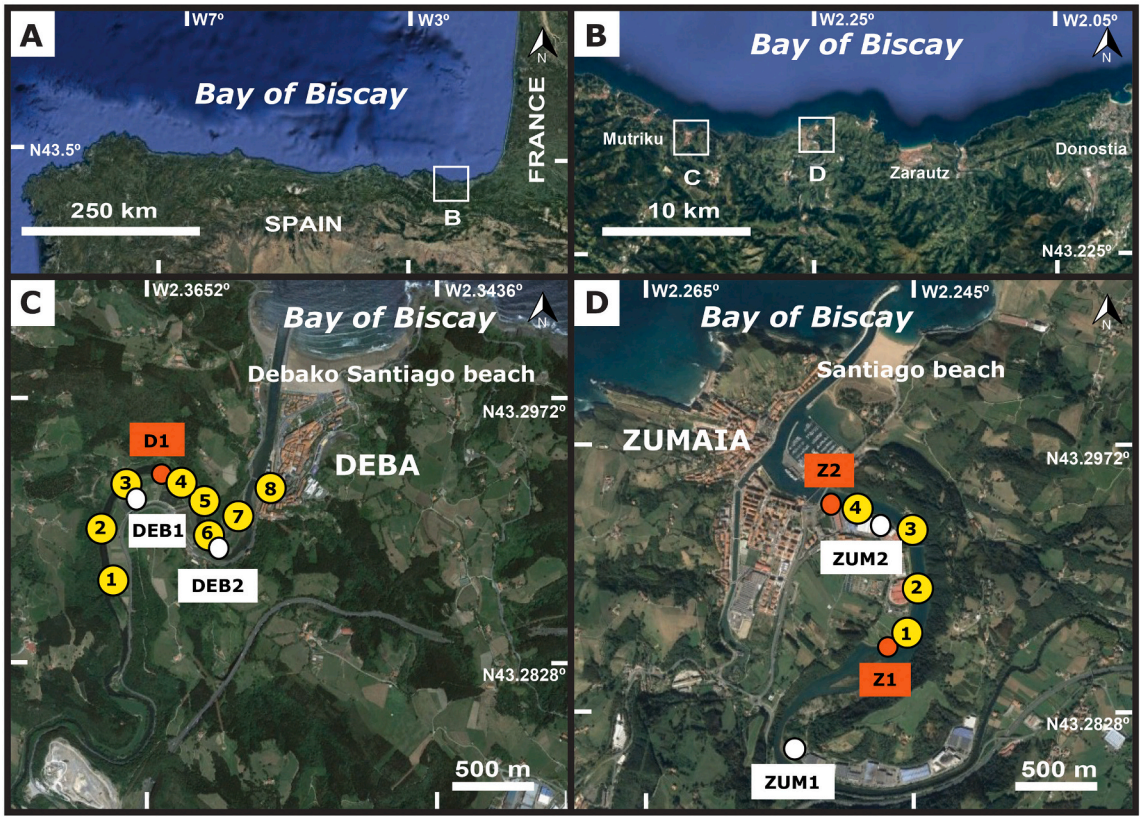

Fig. 1. Geographic location of the Deba and Urola estuaries (Basque Coast Geopark) in the Bay of Biscay (A) and the Eastern Basque coast (B), showing the position of boreholes (white), cores (orange) and surface samples (yellow) (C and D). (For interpretation of the references to colour in this figure legend, the reader is referred to the web version of this article.)

started in 1849 and were completed by 1920 in order to transform the village and its sandy Debako Santiago beach in one of the main summer resorts on the Basque coast. The Deba estuary is a short (5.5 km long), very shallow (0–5 m) and narrow (average 200 m) environment with a total surface of 0.40 km^2 (Villate et al., 1989). Reclamation of salt marshes, originally developed in the middle and upper estuarine areas, initiated in the 17th century but it was particularly intense from the second half of the 19th century, remaining today only 55% of the original estuarine surface (Rivas and Cendrero, 1992). It receives freshwater from a short (63 km) and torrential river (river flow 14 m^3/s) with a very steep water course. Mean annual rainfall in the Deba valley is about 1500 mm, with almost 200 rainy days per year, episodes of >200 mm/day occurring every few years, and a high seasonal variability (Remondo et al., 2003; Rivas et al., 2021). Such a high river flow implies that estuarine salinity values are very low (average 10 PSU in contrast with 34 PSU in littoral waters; Belzunce et al., 2004a), the time needed to replace the volumen of the estuary with freshwater is only 2 h (Borja et al., 2006), and nutrients cannot be processed in this transitional area but are mainly transported to the adjacent coastal waters (Valencia et al., 2004). The mean total suspended solids concentration is 100–130 mg/L and the estimated annual load is 29,300 t/yr, making Deba one of the most turbid rivers on the southern Bay of Biscay (Prego et al., 2008). Differences in river discharges span over two orders of magnitude between low and high flow periods (Lechuga-Crespo et al., 2020) and, given the fast response of the Deba system to precipitation, floods are common events (García-García et al., 2019). This river-dominated estuary is characterised by very abundant coarse-grained fluvial sediments through most of its domains.

The Deba river has been considered as a very polluted setting due to untreated or partially-treated urban and industrial wastewaters discharged for decades (Borja et al., 2006). With more than 125,000 inhabitants and around 1000 large or medium-sized industries located in its fluvial basin, the primary industrial activities are steel and metallurgical plants, automotive plants, galvanizing, smelting and electrical appliance manufacture concentrated around the main urban areas along the river (Montero et al., 2012). Previous works (Belzunce et al., 2004b; Borja et al., 2004; Tueros et al., 2008; Legorburu et al., 2013; Martínez-Santos et al., 2015) found a clear trend of downstream increase in the concentration of diverse trace metals and organic pollutants in sediments and macroinvertebrates, that could be even detected abundantly seaward at 10 m depth in front of the estuary mouth (Legorburu et al., 1989). As a consequence, this transitional area was classified as an environment of "poor ecological quality" (Franco et al., 2004). In order to prevent water pollution, various sewage treatment plants were built during the last twenty years to treat domestic and industrial effluents before they are discharged into the river. As a result, between the years 2000 and 2011 levels of metallic pollution in the Deba estuary showed a general decrease, while the fine sediment stock increased (+11.1%) (Legorburu et al., 2013). Except in 2016, when high concentrations of Cd were detected in one sampling site, between 2014 and 2019 its ecological and chemical status was classified as good (AZTI, 2020). General information on the foraminifera and trace metal content in the recent geological record of the Deba estuary can be found in El bani Altuna et al. (2019).

On the other hand, Zumaia, located 8 km to the east, is a small tourist village founded in 1347 at the mouth of the Urola estuary (Fig. 1). Ironworks and iron trade were important activities along the Urola estuary during the 16th and 18th centuries, and the early construction of port facilities attracted active maritime traffic to Zumaia (Benito Domínguez, 2012). However, sand deposition at the estuary mouth forced to intense dredging since 1914 and the continuous reinforcement of the breakwater dyke and channelling jetty in 1928, 1948 and 1995, favouring in this way accretion of the Santiago beach-dune system (0.05 km^2). The Urola is a short (5.7 km long) and shallow (0–10 m) estuary with a total surface of 0.81 km^2 (Pérez et al., 2009). Reclamation of salt marshes in the inner estuary during the last four centuries occupied 57% of its original surface (Rivas and Cendrero, 1992). It receives freshwater from the short (60 km) and torrential (river flow 8 m^3/s) Urola river that reduces estuarine salinity to 20 PSU and causes a flushing time of 16 h in this tide-dominated estuary (Belzunce et al., 2004a; Borja et al., 2006). In the Urola, the mean total suspended solids concentration is 14–28 mg/L and the estimated annual load is 10,850 t/yr making this river one of the least turbid on the northern Spanish coast (Prego et al., 2008).

The Urola estuary supports a moderate level of anthropogenic pressures, most of them concentrated in the lower estuary. Dredging activities, the presence of a shipyard and a recreational harbour, together with galvanizing and melting industries represent the main human impacts on this environment (Belzunce et al., 2004a). More intense dredging operations have been performed during the last decades in relation to the reinforcement of the estuary mouth, the shipyard activities (initiated in 1921) and the new marina constructed in 1998 behind the Santiago beach-dune system (Fig. 1). Moderate levels of trace metals and organic pollutants in sediments derived from domestic and industrial discharges have also been detected (Legorburu et al., 2013; Tueros et al., 2009). However, a sewage treatment plant located in the middle estuary since 2007 has contributed to the reduction of untreated wastewater discharges into this intertidal system. Between 2000 and 2011 metal stocks accumulated in the Urola estuary decreased but, contrary to that observed in Deba, the fine-grained sediment stock reduced (−32.2%) (Legorburu et al., 2013). Since 2015, its chemical and ecological status has been classified as good (AZTI, 2020).

3. Materials and methods

3.1. Sampling

Two long boreholes and one short core (diameter 10 cm and 16 cm respectively) were retrieved in the Deba estuary. The boreholes DEB1 (upper-middle estuary, X: 551532.17; Y: 4793660.74; Z: +5.53 m; length: 29.4 m) and DEB2 (lower-middle estuary, X: 551884; Y: 4793169; Z: +3.10 m; length: 21 m) were drilled on reclaimed areas using roto-percussion coring until Mesozoic bedrock in 2008 and 2014 respectively. The D1 core (middle estuary, X: 551616; Y: 4793533; Z: +2 m; length: 0.58 m; two replicates) was extracted manually from an intertidal area in 2016. Additionally, eight surface samples were collected along the intertidal estuary in 2017 (Fig. 1). A hard plastic ring was pressed down twice into the surface to obtain samples for micropalaeontological study (1-cm thick, 80 cm^3), while the top millimetres of the sedimentary deposit were scraped off for geochemical analysis.

In the Urola estuary, boreholes ZUM1 (upper estuary, X: 560546; Y: 4792376; Z: +5.71 m; length: 28.2 m) and ZUM2 (lower estuary, X: 561069; Y: 4793612; Z: +3.46 m; length: 25.8 m) were drilled on reclaimed areas in 2014, and cores Z1 (middle estuary, X: 561148; Y: 4792954; Z: +0.62 m; length: 0.47 m; two replicates) and Z2 (lower estuary, X: 560858; Y: 4793713; Z: +0.22 m; length: 0.47 m; two replicates) were obtained from intertidal areas by hand in 2018 and 2015 respectively. Four intertidal surface samples (Fig. 1) were also collected in 2018 following the same procedures used in Deba.

UTM coordinates are referred to the ED50 datum and elevations to the local ordnance datum (LOD: lowest tide at the Bilbao Harbour on 27 September 1878), located 1.73 m below the National Spanish datum at Alicante.

Micropalaeontological (benthic foraminifera) samples were taken at 90-cm intervals approximately in the four long boreholes. Target dry weight was about 300 g and available organic fragments were radiocarbon dated. The three short cores (and their respective duplicates) were divided into 1-cm increments that, once dried in an oven, presented an average weight of 80 g. Trace metals, benthic foraminifera, and natural and artificial radioisotopes were studied from these core samples. All surface samples were analysed for benthic foraminifera and trace metal content, and some of them for radioisotopic activities as well.

3.2. Micropalaeontological and grain-size study

Samples for benthic foraminiferal analysis were sieved with tap water through 2 mm (to avoid large and hard clasts) and 63 μm meshes to remove clay- and silt-size (mud) fractions. In the case of surface samples, the sandy content of the sieve was tipped into a bowl, and an equal volume of Rose Bengal was added for an hour following Walton's (1952) method to differentiate stained forms (alive at the time of collection) from unstained empty tests. These samples were sieved again and washed to remove the excess stain. In all samples, after being dried at 40 °C, foraminifera were concentrated by flotation in trichloroethylene, and the heavy residue was examined for possible unfloated shells. The different foraminiferal assemblages (live, dead and buried) were studied under a stereoscopic binocular microscope using reflected light. Where possible, tests were picked until a representative amount of more than 300 tests per sample was obtained. Otherwise, when foraminifera were scarce, all the available tests were extracted. In total, 194 samples and more than 37,900 foraminiferal tests were studied and taxonomically classified following Loeblich and Tappan (1988) updated in the World Register of Marine Species (WoRMS, http://www.marinespecies.org/foraminifera). The abundance of foraminifera is expressed as the number of individuals/80 cm^3 (standing crop) in the case of live assemblages from the surface samples, and as the number of tests/15 g of sediment for the buried assemblages of the core samples. Abundance results are gathered also into qualitative groups (very low, low, moderate, high, and very high) following the foraminiferal quantification of absolute and relative abundances of tests and species for estuaries in northern Spain by García-Artola et al. (2016). In order to enable samples containing different number of individuals to be compared a diversity index has been used. The Fisher alpha index was first described by Fisher et al. (1943) to understand the relationship between the number of species and the number of individuals in a random sample. Only those samples from which at least 100 tests were counted have been used because smaller numbers are not considered sufficiently reliable for determination of the value. There is a clear relationship between the diversity of a foraminiferal assemblage and the nature of its environment. In a general sense, alpha =5 is a boundary separating normal marine environments (alpha >5) from marginal environments (alpha <5) (Murray, 2006). Foraminiferal assemblages were identified based on the presence, abundance and dominance of the different taxa. The percentage of each species within the assemblages was calculated considering as representative only those samples that contained more than 100 tests. Species were classified into estuarine or autochthonous (taxa that live and reproduce in the estuary) and marine or allochthonous (species living in the inner shelf and transported into the estuary) based on their modern distribution from nearby estuarine environments of northeastern Spain (Cearreta, 1988; Cearreta et al., 2002a). All the foraminiferal species identified in the samples are listed in Table A1.

Grain size was determined during sample preparation for foraminiferal analysis, as the gravel- and sand-size fractions were retained on the 2 mm and 63 μm sieves respectively.

3.3. Geochemical study

Sediment samples (<2 mm) from short cores and surface samples were mechanically homogenised using an agate mortar and pestle for their trace metal geochemical analysis. Elemental concentrations were analysed in Activation Laboratories Ltd. (Ontario, Canada) by Inductively Coupled Plasma-Optical Emission Spectrometry (ICP-OES) after digestion of a 0.5-g sample using aqua regia for 2 h at 95 °C. Detection limits were 0.01% for Al, 2 mg/kg for Zn and Pb, and 1 mg/kg for Cu, Cr and Ni.

When dealing with estuarine sediments, normalisation of trace metal concentrations to the content of a conservative element such as Al is an extended practice in order to compensate for the potential effects of granulometric and mineralogical differences (e.g., Horowitz, 1985; Santschi et al., 2001; Ho et al., 2012). However, as Al-normalisation does not lead to substantial changes in the geochemical profiles of the analysed cores, results have been represented here as raw data. Furthermore, in order to assess the environmental impact derived from the accumulation of trace metals we have used, as accurate non-regulatory benchmarks for comparison, the Spanish guidelines for the characterisation of dredged material and its subsequent relocation within waters of the maritime-terrestrial public domain (Buceta et al., 2015; Comisión Interministerial de Estrategias Marinas, 2015). According to this proposal, when concentrations in the fraction <2 mm remain below the Action Level B (410, 218, 168, 340 and 63 mg/kg for Zn, Pb, Cu, Cr and Ni respectively), they are supposed to not have statistically significant biological effects. In turn, the content between Action Level B and C (1640, 600, 675, 1000 and 234 mg/kg for Zn, Pb, Cu, Cr and Ni respectively) represents the range in which there is uncertainty about their possible effects on biota, which should be resolved by conducting bioassays. Sediments with chemicals at or above the Action Level C are considered polluted and they are not suitable for unconfined, open water disposal.

Different microscopic spheroidal particles were identified in the Urola short cores and their variable composition was analysed by SEM-EDX (scanning electron microscopy energy dispersive X-ray spectroscopy) at the University of the Basque Country UPV/EHU (Spain).

3.4. Radiometric study

Forty four samples of wood fragments, plant debris and marine shells from the boreholes were radiocarbon dated (Accelerator Mass Spectrometry, AMS or radiometric) at Beta Analytic (USA). Terrestrial and marine materials were calibrated using the IntCal20 (Reimer et al., 2020) and Marine20 (Heaton et al., 2020) calibration curves respectively with CLAM package in "R" (Blaauw, 2010). Ages are reported with a 2σ error (95% confidence interval) and expressed as calibrated years before present (yr cal BP), where zero is 1950 CE (Table A2). Median probability values are used throughout the manuscript to report ages of the lower and upper boundaries for each unit.

Specific activities of both natural (^{210}Pb and ^{226}Ra) and artificial (^{137}Cs) short-lived radiotracers were measured in samples from the cores and few surface samples. An evaluation of sedimentation rates and their temporal evolution was carried out, as well as an estimation of the chronology of the different units. Dating of recent sedimentary records is based on the vertical distribution of the ^{210}Pb concentrations using ^{137}Cs as possible validation. The method is founded on the activity of the deposited atmospheric $^{210}Pb_{xs}$, denominated in excess, that results from the difference between the total ^{210}Pb measured and that fraction of the same radioisotope derived from the ^{226}Ra present in the sediments, called ^{210}Pb in equilibrium (Appleby and Oldfield, 1992). All concentrations have been determined at the University of Cantabria (Spain) by gamma spectrometry, using a low-background high purity HPGe detector (see complete procedural details in Álvarez-Iglesias et al., 2007 and Cearreta et al., 2013).

Since the concentration of $^{210}Pb_{xs}$ is cancelled at a certain depth, chronologies and evolution of sediment accumulation rates with time were established by applying the constant rate of supply (CRS) model in cores D1 and Z2. This model assumes a constant flux of unsupported ^{210}Pb to the sediment and allows the rate of sedimentation to vary over time. The initial concentration of $^{210}Pb_{xs}$ is inversely proportional to the sedimentation rate and it can be estimated from the complete inventory. On the other side, exponential decrease of $^{210}Pb_{xs}$ with depth in core Z1 reflects constant ^{210}Pb flux and sedimentation rates and, therefore, the constant flux/constant sedimentation (CFCS) model was applied to this record (e.g., Krishnaswamy et al., 1971; Robbins, 1978; Appleby and Oldfield, 1978, 1983; Sanchez-Cabeza and Ruiz-Fernández, 2012).

4. Results

4.1. Holocene boreholes

4.1.1. Borehole DEB1

Based on its micropalaeontological content, three different units were distinguished in this borehole (Fig. 2, Table 1). Above the basement, Unit 1 (−23.8/−17.3 m, dated between >9800 and 9000 yr cal BP) is a sandy and gravelly mud interval dominated by the foraminiferal species *Ammonia tepida* (average 39%) and *Haynesina germanica* (33%), with *Rosalina irregularis* (8%) and *Cribroelphidium williamsoni* (7%) as secondary taxa. Marine allochthonous tests represented up to 20% of the foraminiferal assemblage (average 10%, mainly *R. irregularis*, *Miliolinella subrotunda*, *Cibicidoides lobatulus* and *Bolivina variabilis*). This unit contains the highest number of species in this borehole (average 9 species, alpha 1.82) and it is interpreted as a muddy, brackish intertidal environment with marine influence. Unit 2 (−17.3/−1.5 m, 9000 to <6700 yr cal BP) is characterised by muddy sand with bioclasts, with *H. germanica* (46%), *A. tepida* (37%) and *C. williamsoni* (15%) as main taxa. The average number of species is 6 (alpha 1.29) and allochthonous tests are very scarce (0.7%). This interval represents sandy, brackish intertidal conditions with limited marine influence. Final Unit 3 (−1.5/+5.3 m), made of gravelly sand, is barren of foraminifera and grain size is greater than in the previous units. Consequently, it is considered as deposited under fluvial conditions that prevented the development of saline-affinity organisms, such as foraminifera.

4.1.2. Borehole DEB2

This borehole exhibits three units based on its foraminiferal contents (Fig. 2, Table 1). Basal Unit 1 (−17.9/−13.6 m, >8800 to 8800 yr cal BP) is the interval with the highest number of species (average 12 species, alpha 2.63), among which *A. tepida* (41%), *H. germanica* (36%) and *C. williamsoni* (12%) are dominant. This environment of muddy and gravelly sand with bioclasts was deposited under sandy, brackish

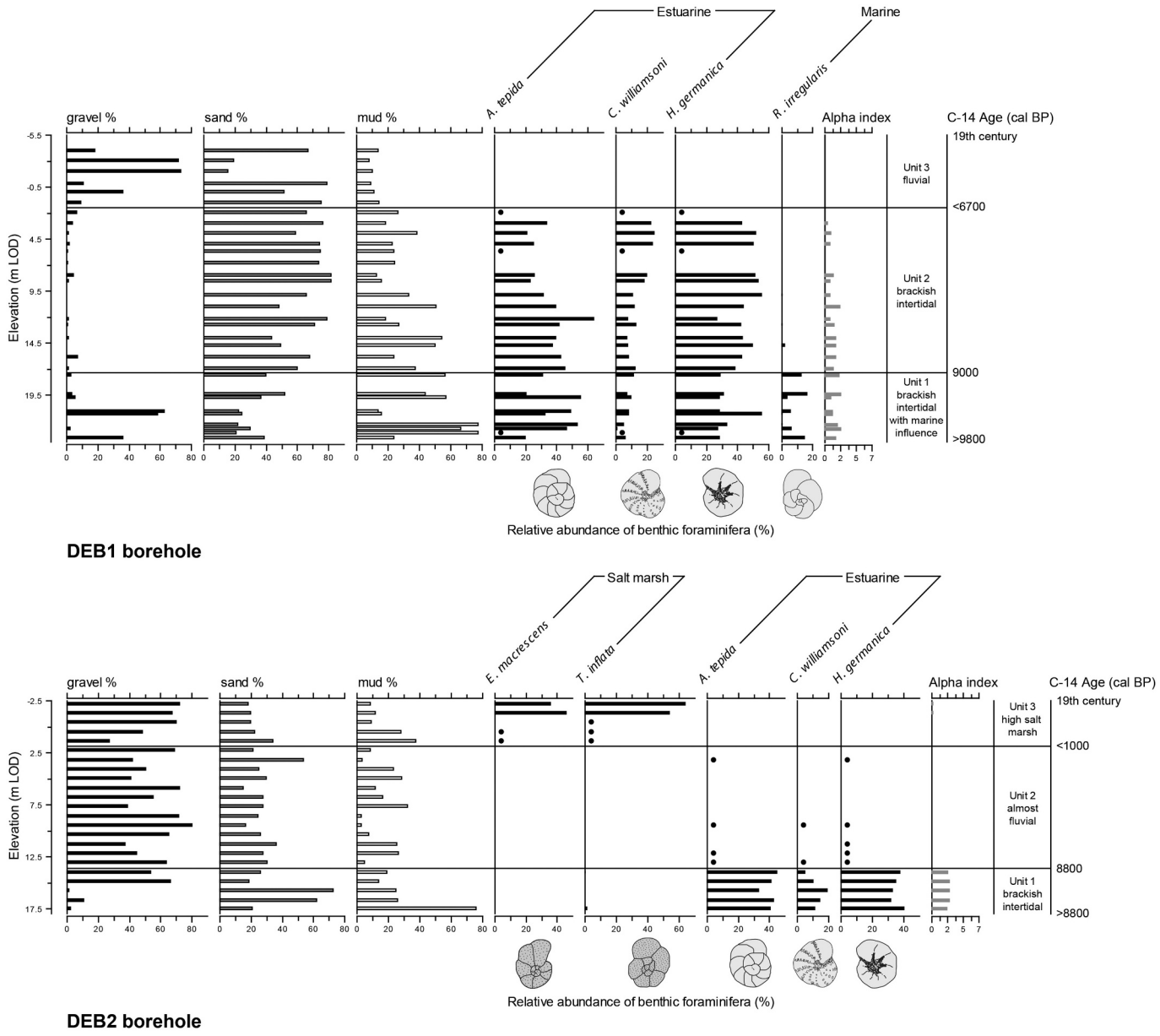

Fig. 2. Vertical distribution of grain size (%), relative abundance of main foraminiferal species (%), alpha diversity index, depositional environment and C-14 age (median values of calibrated radiocarbon dates) with depth (m) in boreholes DEB1 and DEB2, Deba estuary (Basque Coast Geopark). Black dots indicate presence of the species in assemblages with less than 100 foraminiferal tests.

Table 1
Summary of lithological, age and microfaunal data from boreholes drilled in the Deba and Urola estuaries (Basque Coast Geopark). The single value represents the average and those in parentheses give the range. The age corresponds to median values of calibrated radiocarbon dates.

DEB1 borehole				
Unit 1	Unit 2	Unit 3		
Elevation −23.8/−17.3 m LOD	Elevation −17.3/−1.5 m LOD	Elevation −1.5/+5.3 m LOD		
Thickness 6.5 m	Thickness 15.8 m	Thickness 7.0 m		
Lithology: sandy and gravelly mud	Lithology: muddy sand with bioclasts	Lithology: gravelly sand		
Mud 48 (14–78)%	Mud 30 (13–55)%	Mud 12 (1–15)%		
Sand 32 (21–52)%	Sand 67 (44–82)%	Sand 51 (16–79)%		
Gravel 20 (0–63)%	Gravel 3 (0–8)%	Gravel 37 (10–74)%		
No. species 9 (4–12)	No. species 6 (3–9)	No foraminifera		
Alpha index 1.82 (1.06–2.49)	Alpha index 1.29 (0.46–2.39)			
Marine tests 10 (0−20)%	Marine tests 0.7 (0–2)%			
Hyaline 96%	Hyaline 99.5%			
Porcellaneous 4%	Porcellaneous 0.5%			
Agglutinated 0%	Agglutinated 0%			
A. tepida 39 (20–55)%	*H. germanica* 46 (25–57)%			
H. germanica 33 (27–55)%	*A. tepida* 37 (21–64)%			
R. irregularis 8 (0–17)%	*C. williamsoni* 15 (8–24)%			
C. williamsoni 7 (1−11)%				
Palaeoenvironment: muddy, brackish intertidal	Palaeoenvironment: sandy, brackish intertidal	Palaeoenvironment: fluvial		
C-14 Age: >9800 / 9000 cal BP	C-14 Age: 9000 / <6700 cal BP	C-14 Age: <6700 cal BP / 19th century		
DEB2 borehole				
Unit 1	Unit 2	Unit 3		
Elevation −17.9/−13.6 m LOD	Elevation −13.6/−1.9 m LOD	Elevation −1.9/+2.2 m LOD		
Thickness 4.3 m	Thickness 11.7 m	Thickness 4.1 m		
Lithology: muddy and gravelly sand with bioclasts	Lithology: sandy and muddy gravel	Lithology: sandy and muddy gravel		
Mud 32 (14–76)%	Mud 15 (3−32)%	Mud 24 (9–29)%		
Sand 40 (19–73)%	Sand 28 (16–54)%	Sand 29 (19–34)%		
Gravel 28 (2–67)%	Gravel 57 (38–80)%	Gravel 57 (28–72)%		
No. species 12 (10−13)	No foraminifera	No. species 2 (1–2)		
Alpha index 2.63 (2.44–2.76)		Alpha index 0.29		
Marine tests 6 (4–9)%		Marine tests 0%		
Hyaline 97%		Hyaline 0%		
Porcellaneous 2%		Porcellaneous 0%		
Agglutinated 1%		Agglutinated 100%		
A. tepida 41 (34–45)%		T. inflata 59 (54-64)%		
H. germanica 36 (32–40)%		E. macrescens 41 (36-46)%		
C. williamsoni 12 (6–19)%				
Palaeoenvironment: sandy, brackish intertidal	Palaeoenvironment: fluvial	Palaeoenvironment: gravelly, high salt marsh		
C-14 Age: >8800 / 8800 cal BP	C-14 Age: 8800 / <1100 cal BP	C-14 Age: <1100 cal BP / 19th century		
ZUM1 borehole				
Unit 1	Unit 2	Unit 3	Unit 4	
Elevation −22.0/−15.7 m LOD	Elevation −15.7/−5.8 m LOD	Elevation −5.8/−3.1 m LOD	Elevation −3.1/−1.0 m LOD	
Thickness 6.3 m	Thickness 9.9 m	Thickness 2.7 m	Thickness 2.1 m	
Lithology: gravelly and muddy sand	Lithology: gravelly and muddy sand	Lithology: sandy gravel	Lithology: sandy mud	
Mud 23 (15–31)%	Mud 24 (9–64)%	Mud 7 (5–10)%%	Mud 77 (63–89)%	
Sand 54 (17–72)%	Sand 45 (28–71)%	Sand 40 (24–69)%	Sand 21 (11−33)%	
Gravel 23 (2–63)%	Gravel 31 (1–61)%	Gravel 53 (21–71)%	Gravel 2 (0–3)%	
No foraminifera	No. species 11 (4–20)	Few foraminifera	No. species 7 (6–10)	
	Alpha index 2.17 (1.36–3.69)		Alpha index 1.42 (0.98–1.98)	
	Marine tests 2 (0–4)%		Marine tests 0%	
	Hyaline 99%		Hyaline 7%	
	Porcellaneous 0%		Porcellaneous 0%	
	Agglutinated 1%		Agglutinated 93%	
	H. germanica 33 (18–46)%		*T. inflata* 50 (46–53)%	
	C. williamsoni 29 (17–60)%		*E. macrescens* 32 (21–42)%	
	A. tepida 28 (9–41)%		*A. tepida* 6 (1–15)%	
	E. oceanense 5 (1−12)%			
Palaeoenvironment: fluvial	Palaeoenvironment: sandy, brackish intertidal	Palaeoenvironment: almost fluvial	Palaeoenvironment: muddy, low salt marsh	
C-14 Age: >11,100 / 8700 cal BP	C-14 Age: 8700 / <6200 cal BP	C-14 Age: <6200 / 1200 cal BP	C-14 Age: 1200 cal BP / <16th century	
ZUM2 borehole				
Unit 1	Unit 2	Unit 3	Unit 4	Unit 5
Elevation −22.3/−20.4 m LOD	Elevation −20.4/−14.1 m LOD	Elevation −14.1/−6.1 m LOD	Elevation −6.1/−2.5 m LOD	Elevation −2.5/−1.2 m LOD
Thickness 1.9 m	Thickness 6.3 m	Thickness 8.0 m	Thickness 3.6 m	Thickness 1.3 m
Lithology: sandy and muddy	Lithology: sand with bioclasts	Lithology: slightly muddy sand	Lithology: muddy sand	Lithology: mud

(*continued on next page*)

Table 1 (*continued*)

DEB1 borehole				
Unit 1	Unit 2	Unit 3		
gravel	Mud 6 (2–17)%	with bioclasts	Mud 36 (22–50)%	Mud 90 (87–92)%
Mud 23 (17–29)%	Sand 93 (82–98)%	Mud 13 (4–35)%%	Sand 63 (49–77)%	Sand 9 (8–12)%
Sand 36 (25–48)%	Gravel 1 (0–4)%	Sand 86 (63–95)%	Gravel 1 (0–1)%	Gravel 1 (0–1)%
Gravel 41 (36–46)%		Gravel 1 (0–3)%		
No foraminifera	No. species 15 (12–19)	No. species 18 (14–24)	No. species 13 (9–19)	No. species 3 (2–3)
	Alpha index 3.42 (2.45–4.16)	Alpha index 4.66 (3.41–5.96)	Alpha index 2.60 (1.73–3.98)	Alpha index 0.57
	Marine tests 96 (88–99)%	Marine tests 51 (17–88)%	Marine tests 7 (4–10)%	Marine tests 0%
	Hyaline 76%	Hyaline 87%	Hyaline 100%	Hyaline 8%
	Porcellaneous 9%	Porcellaneous 9%	Porcellaneous 0%	Porcellaneous 0%
	Agglutinated 15%	Agglutinated 4%	Agglutinated 0%	Agglutinated 92%
	C. lobatulus 62 (58–69)%	*C. lobatulus* 31 (5–66)%	*A. tepida* 41 (37–48)%	*T. inflata* 77%
	C. rudis 13 (11–16)%	*A. tepida* 24 (2–43)%	*H. germanica* 39 (33–50)%	*E. macrescens* 18%
	E. crispum 9 (2–14)%	*H. germanica* 17 (2–29)%	*C. williamsoni* 11 (9–16)%	*H. germanica* 5%
		C. williamsoni 5 (0−10)%		
Palaeoenvironment: fluvial	Palaeoenvironment: sandy, near marine intertidal	Palaeoenvironment: sandy, brackish intertidal	Palaeoenvironment: sandy, brackish intertidal	Palaeoenvironment: muddy, low salt marsh
	C-14 Age: >9100 / 8300 cal BP	C-14 Age: 8300 / 7300 cal BP	C-14 Age: 7300 / 6700 cal BP	C-14 Age: 6700 cal BP / <16th century

LOD: local ordnance datum.

intertidal conditions. Despite its indicative value of scarce marine influence (allochthonous tests represent only 6% on average), younger environmental conditions registered in this geological record are even more restricted. Above, Unit 2 (−13.6/−1.9 m) is made of sandy and muddy gravel containing few foraminifera. Coarse grain size and extremely scarce foraminifera are indicative of a fluvial environment deposited between 8800 and < 1100 yr cal BP. Lastly, foraminiferal numbers increase upwards in Unit 3 (−1.9/+2.2 m), although only two agglutinated species (alpha 0.29) are present: *Trochammina inflata* (59%) and *Entzia macrescens* (41%). These are typical of a high salt

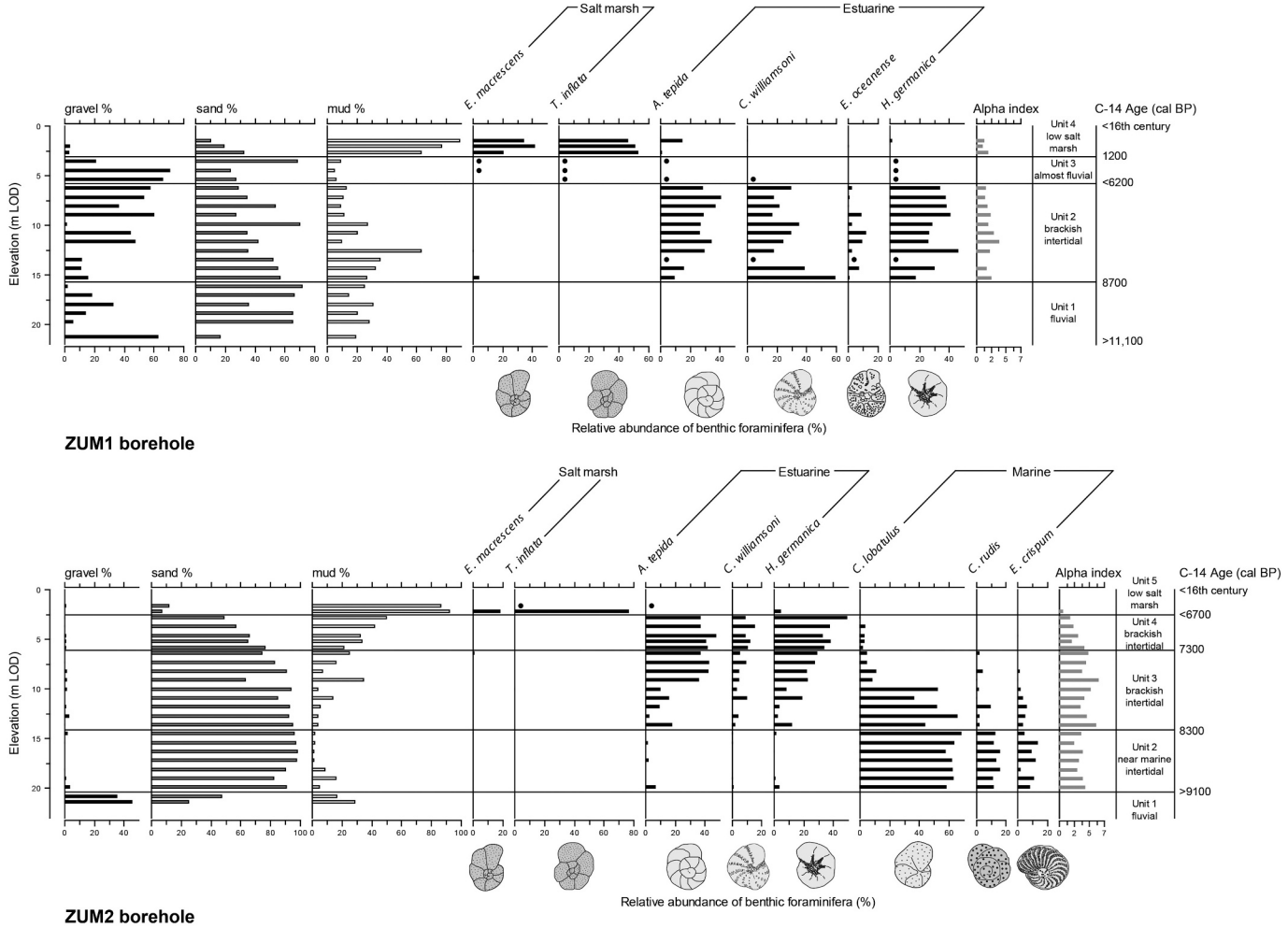

Fig. 3. Vertical distribution of grain size (%), relative abundance of main foraminiferal species (%), alpha diversity index, depositional environment and C-14 age (median values of calibrated radiocarbon dates) with depth (m) in boreholes ZUM1 and ZUM2, Urola estuary (Basque Coast Geopark). Black dots indicate presence of the species in assemblages with less than 100 foraminiferal tests.

marsh environment that implies vegetated, highly restricted, extreme tidal conditions.

4.1.3. Borehole ZUM1

This borehole contains four different units (Fig. 3, Table 1). Unit 1 (−22.0/−15.7 m, >11,100 to 8700 yr cal BP) is located above the rocky basement and is barren of foraminiferal tests. This gravelly and muddy sand interval is interpreted as a fluvial environment. Following Unit 2 (−15.7/−5.8 m) is made of gravelly and muddy sand with a moderate number of species (11 species, alpha 2.17) and a very low content of allochthonous tests (2%). Foraminiferal assemblage is dominated by *H. germanica* (33%), *C. williamsoni* (29%) and *A. tepida* (28%) with secondary *Elphidium oceanense* (5%). This unit was deposited under sandy, brackish intertidal, very restricted conditions developed in the

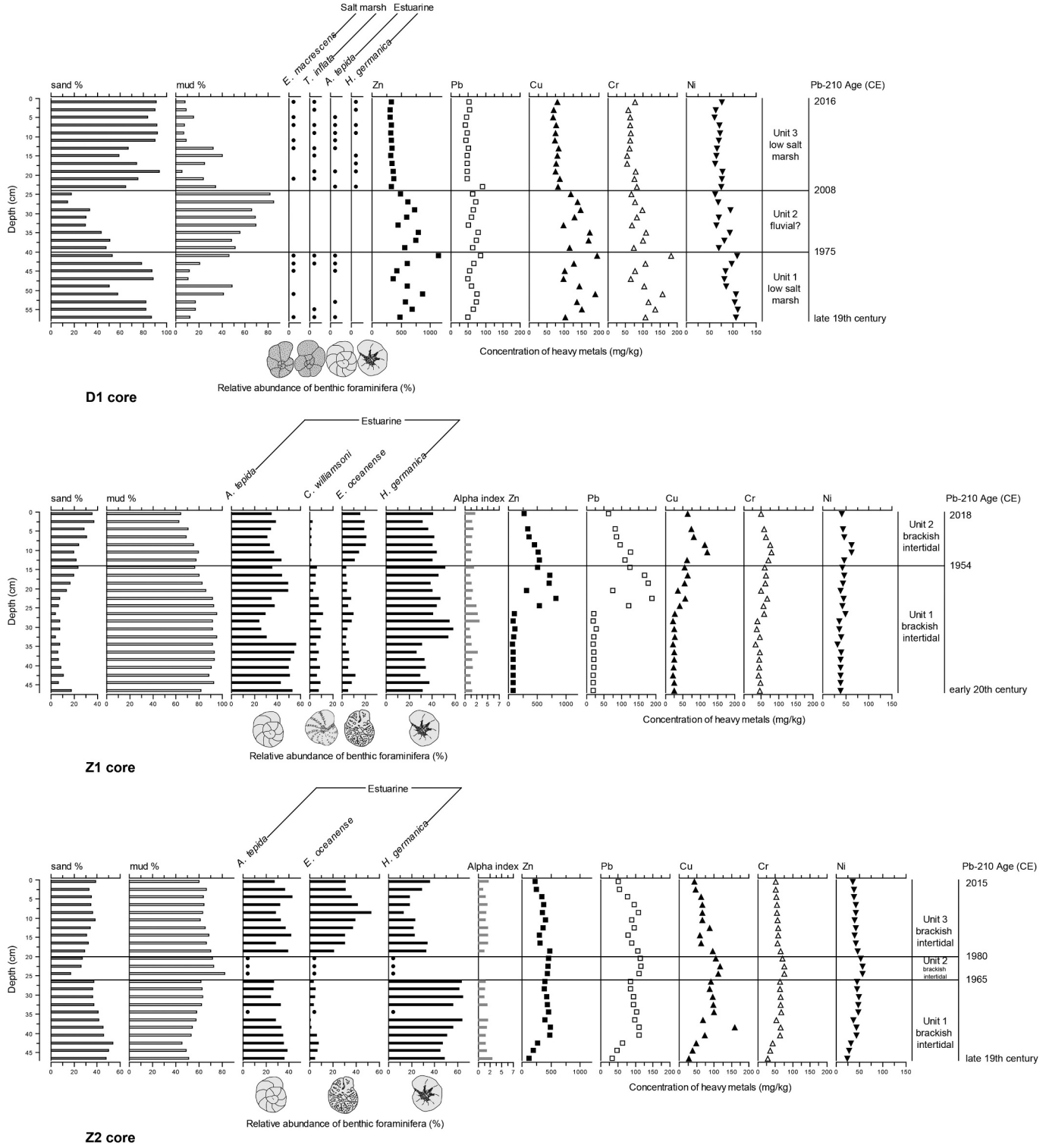

Fig. 4. Distribution of grain size (%), trace metals (mg/kg), relative abundance of main foraminiferal species (%), alpha diversity index, depositional environment and Pb-210 age (CE) with depth (cm) in cores D1, Z1 and Z2, Deba and Urola estuaries (Basque Coast Geopark). Black dots indicate presence of the species in assemblages with less than 100 foraminiferal tests.

Table 2
Summary of lithological, microfaunal, age and geochemical data from cores retrieved in the Deba and Urola estuaries (Basque Coast Geopark). The single value represents the average and those in parentheses give the range.

D1 core		
Unit 1	Unit 2	Unit 3
Depth interval 58/40 cm	Depth interval 40/24 cm	Depth interval 24/0 cm
Thickness 18 cm	Thickness 16 cm	Thickness 24 cm
Lithology: muddy sand	Lithology: sandy mud	Lithology: muddy sand
Mud 26 (11–49)%	Mud 66 (49–85)%	Mud 18 (6–41)%
Sand 74 (51–89)%	Sand 34 (15–52)%	Sand 82 (60–94)%
Zn 645 (366–1150) mg/kg	Zn 627 (457–797) mg/kg	Zn 340 (315–381) mg/kg
Pb 65 (50–87) mg/kg	Pb 67 (52–79) mg/kg	Pb 52 (42–92) mg/kg
Cu 139 (99–195) mg/kg	Cu 137 (99–173) mg/kg	Cu 78 (68–88) mg/kg
Cr 117 (65–182) mg/kg	Cr 85 (69–110) mg/kg	Cr 67 (54–84) mg/kg
Ni 99 (82–111) mg/kg	Ni 76 (65–95) mg/kg	Ni 70 (61–77) mg/kg
Few foraminifera	No foraminifera	Few foraminifera
No. tests/15 g: 1 (0–2)		No. tests/15 g: 2 (1–5)
Palaeoenvironment: sandy, low salt marsh	Palaeoenvironment: fluvial	Palaeoenvironment: sandy, low salt marsh
Pb-210 Age: late 19th century-1975 CE	Pb-210 Age: 1975–2008 CE	Pb-210 Age: 2008–2016 CE
Z1 core		
Unit 1	Unit 2	
Depth interval 47/14 cm	Depth interval 14/0 cm	
Thickness 33 cm	Thickness 14 cm	
Lithology: sandy mud	Lithology: sandy mud	
Mud 90 (77–96)%	Mud 72 (63–80)%	
Sand 10 (4–24)%	Sand 28 (20–37)%	
Zn 244 (83–827) mg/kg	Zn 415 (276–541) mg/kg	
Pb 64 (19–190) mg/kg	Pb 95 (64–127) mg/kg	
Cu 33 (21–63) mg/kg	Cu 86 (62–120) mg/kg	
Cr 50 (34–67) mg/kg	Cr 66 (49–80) mg/kg	
Ni 40 (32–49) mg/kg	Ni 51 (41–62) mg/kg	
Carbonaceous spheroids	Carbonaceous spheroids	
	Polymeric spheroids	
No. species 9 (6–14)	No. species 8 (6–10)	
Alpha index 1.74 (1.03–3.04)	Alpha index 1.59 (1.28–2.17)	
No. tests/15 g: 116 (49–181)	No. tests/15 g: 62 (34–90)	
Marine tests 1 (0–5)%	Marine tests 1 (0–3)%	
Agglutinated 1%	Agglutinated 1%	
Porcellaneous 1%	Porcellaneous 1%	
Hyaline 98%	Hyaline 98%	
A. tepida 42 (25–56)%	*H. germanica* 39 (32–44)%	
H. germanica 41 (27–58)%	*A. tepida* 36 (32–44)%	
C. williamsoni 7 (3−12)%	*E. oceanense* 17 (11−21)%	
E. oceanense 6 (3−11)%		
Palaeoenvironment: muddy, brackish intertidal	Palaeoenvironment: muddy, brackish intertidal	
Pb-210 Age: early 20th century-1954 CE	Pb-210 Age: 1954–2018 CE	
Z2 core		
Unit 1	Unit 2	Unit 3
Depth interval 47/26 cm	Depth interval 26/20 cm	Depth interval 20/0 cm
Thickness 21 cm	Thickness 6 cm	Thickness 20 cm
Lithology: sandy mud	Lithology: sandy mud	Lithology: sandy mud
Mud 57 (46–64)%	Mud 76 (72–83)%	Mud 65 (61–70)%
Sand 43 (37–54)%	Sand 24 (17–28)%	Sand 35 (30–39)%
Zn 374 (128–493) mg/kg	Zn 451 (439–461) mg/kg	Zn 343 (227–488) mg/kg
Pb 85 (33−112) mg/kg	Pb 114 (112–116) mg/kg	Pb 86 (51–109) mg/kg
Cu 81 (28–159) mg/kg	Cu 112 (106–117) mg/kg	Cu 66 (44–96) mg/kg
Cr 56 (28–67) mg/kg	Cr 74 (70–76) mg/kg	Cr 56 (51–66) mg/kg
Ni 40 (24–49) mg/kg	Ni 55 (52–56) mg/kg	Ni 40 (35–46) mg/kg
Carbonaceous spheroids	Iron spheroids	Polymeric spheroids
	Carbonaceous spheroids	Iron spheroids
		Carbonaceous spheroids
No. species 9 (6–14)	Few foraminifera	No. species 9 (6–11)
Alpha index 1.74 (1.26–2.93)	No. tests/15 g: 15 (9–21)	Alpha index 1.70 (1.05–2.19)
No. tests/15 g: 156 (21–518)		No. tests/15 g: 166 (38–280)
Marine tests 2 (1–4)%		Marine tests 1 (0–2)%
Agglutinated 2%		Agglutinated 1%
Porcellaneous 0%		Porcellaneous 2%
Hyaline 98%		Hyaline 97%
H. germanica 56 (45–65)%		*E. oceanense* 35 (21–53)%
A. tepida 32 (24–39)%		*A. tepida* 35 (27–43)%
E. oceanense 5 (1–8)%		*H. germanica* 25 (14–36)%
Palaeoenvironment: muddy, brackish intertidal	Palaeoenvironment: muddy, brackish intertidal	Palaeoenvironment: muddy, brackish intertidal
Pb-210 Age: late 19th century-1965 CE	Pb-210 Age: 1965–1980 CE	Pb-210 Age: 1980–2015 CE

upper estuary between 8700 and < 6200 yr cal BP. Unit 3 (−5.8/−3.1 m) is a sandy gravel interval containing few foraminiferal tests and deposited under mainly fresh water conditions from <6200 to 1200 yr cal BP. Finally, sandy mud accumulated between 1200 yr cal BP and the 16th century constitutes Unit 4 (−3.1/−1.0 m). It is dominated by agglutinated foraminifera with a low number of species (7 species, alpha 1.42), no marine tests, and *T. inflata* (50%) and *E. macrescens* (32%) as dominant species together with *A. tepida* (6%) as a secondary taxon. Its depositional environment was a muddy, low salt marsh.

4.1.4. Borehole ZUM2

Five units have been differentiated above the basement in this borehole from the Urola estuary (Fig. 3, Table 1). Firstly, basal Unit 1 (−22.3/−20.4 m) contains no foraminifera in this sandy and muddy gravel interval that is considered as deposited in a fluvial environment. The following Unit 2 (−20.4/−14.1 m, >9100 to 8300 yr cal BP) is made of sand with bioclasts dominated by the allochthonous species *C. lobatulus* (62%), *Connemarella rudis* (13%) and *Elphidium crispum* (9%). Marine tests are highly dominant (96%) in this foraminiferal assemblage. The number of species is high (15 species, alpha 3.42) and the agglutinated (15%) and porcellaneous (9%) wall type content are moderate. It is interpreted as a sandy, near marine intertidal environment. Unit 3 (−14.1/−6.1 m, between 8300 and 7300 yr cal BP) contains *C. lobatulus* (31%), *A. tepida* (24%) and *H. germanica* (17%) as main taxa. *Cribroelphidium williamsoni* is a secondary species (5%). This slightly muddy sand unit presents a high number of species (18 species, alpha 4.66) and marine tests (average 51% decreasing upwards), and a moderate abundance of porcellaneous shells (9%). This interval was accumulated under sandy, brackish intertidal conditions with a significative influence of the open sea. Above, Unit 4 (−6.1/−2.5 m) is made of muddy sand deposited between 7300 and 6700 yr cal BP. It is dominated by *A. tepida* (41%), *H. germanica* (39%) and *C. williamsoni* (11%), with a moderate number of species (13 species, alpha 2.60) and a reduced content of marine tests (7%). Its depositional environment was sandy and more restricted, brackish intertidal. Finally, muddy Unit 5 (−2.5/−1.2 m) contains very few species (3 species, alpha 0.57), no marine tests, and a foraminiferal assemblage dominated by *T. inflata* (77%) and *E. macrescens* (18%), with secondary *H. germanica* (5%). This is indicative of a low salt marsh environment developed during the last millennia until the reclamation of the area around the 16th century.

4.2. Recent cores

4.2.1. Core D1

Despite the very low abundance of foraminifera, that did not allow calculation of species relative abundance, three different units could be distinguished in this core based on its microfossil and geochemical contents (Fig. 4, Table 2). Unit 1 (58/40 cm) is the lower muddy sand interval that contains only three agglutinated and hyaline taxa: *E. macrescens* (19 tests), *T. inflata* (10 tests) and *A. tepida* (6 tests). The number of foraminifera is extremely low (average 1 test/15 g). This unit is interpreted as a sandy, low salt marsh. Middle Unit 2 (40/24 cm) is made of sandy mud barren of foraminifera, probably as a consequence of the great influence of fresh water. Finally, the uppermost 24 cm of muddy sand (Unit 3) contain a slightly greater presence of foraminiferal tests (2 tests/15 g) and species number (4 species): *T. inflata* (25 tests), *H. germanica* (20 tests), *A. tepida* (13 tests) and *E. macrescens* (9 tests). This mixture of agglutinated and hyaline tests is interpreted as a brackish intertidal low salt marsh environment.

Vertical profiles displayed by trace metals are fairly similar (Fig. 4). They exhibit variable concentrations throughout Units 1 and 2 (Table 2), clearly higher than those proposed by Rodríguez et al. (2006) as geochemical background for estuarine and coastal sediments from the Basque Country (147, 31, 33, 26 and 29 mg/kg for Zn, Pb, Cu, Cr and Ni respectively). The highest values of Zn (1150 mg/kg), Cu (195 mg/kg), Cr (182 mg/kg) and Ni (109 mg/kg) appear at the boundary between Unit 1 and Unit 2, at 40 cm depth. Along Unit 3 concentrations of trace metals remain relatively low and almost constant, except for the marked peak in Pb observed in the lowest sample (92 mg/kg at 24–22 cm depth). Distribution of $^{210}Pb_{xs}$ activities with depth shows a decreasing trend throughout Units 2 and 1, nearly achieving equilibrium in bottom samples (Fig. 5). However, contrary to expected, sediments from Unit 3 exhibit extremely low concentrations, reaching values close to zero in two samples. The most likely explanation for this apparent depletion is that the top 24 cm have received the input of older sediments and/or imported materials that do not normally belong to this environment. They probably derived from the construction and maintenance of the infrastructures performed in this middle estuarine area during recent years (e.g., a bridge and a tunnel for the road connection between the towns of Deba and nearby Mutriku, inaugurated in 2006, and restoration works developed later in the surrounding area). This hypothesis would be supported by the average concentration of $^{210}Pb_{xs}$ (38 Bq/kg) obtained from three surface samples collected close to the core (stations Deba-3, 4 and 5), which is well above the content found in Unit 3 (0.36–9.40 Bq/kg) and moderately above the $^{210}Pb_{xs}$ activity measured in the first two cm of Unit 2 (28.3 Bq/kg). Moreover, trace metals exhibit a similar behaviour, since contents of most of them in nearby surface sediments (see Table 3) and in Units 1 and 2 are also in excess of the almost constant values determined throughout Unit 3 (Table 2).

Application of the CRS model provided a chronological framework for this core: Unit 1 can be dated between the end of the 19th century and 1975 CE, Unit 2 was deposited between 1975 and 2008 CE and Unit 3 accumulated between 2008 and 2016 CE (Table 2). Unfortunately, the concentrations of ^{137}Cs did not provide significant information to validate the proposed ages, as no clear maximum along the entire profile is observed (Fig. 5). Regarding sediment accumulation rates, they exhibit an increasing trend with time (Fig. 5). After a moderate peak in the mid-1970s, when they rise from <0.4 to 1.12 cm/yr, dramatically high and variable values (2.35- > 5 cm/yr) are determined since 2008 CE (Unit 3). They are likely to reflect the episodic arrival of increased amounts of materials as a result of the anthropogenic interventions developed recently in the surrounding area.

4.2.2. Core Z1

Two different units have been identified in this core (Fig. 4, Table 2). A lower Unit 1 (47/14 cm) contains a high number of foraminiferal tests (116 tests/15 g) and a moderate number of species (9 species, alpha 1.74), and is dominated by the hyaline forms *A. tepida* (42%) and *H. germanica* (41%), with *C. williamsoni* (7%) and *E. oceanense* (6%) as secondary taxa. The abundance of marine tests is minimal (1%) in this sandy mud interval deposited under brackish conditions. Additionally, spherical carbonaceous particles were encountered in great abundance in this basal Unit 1. Above, Unit 2 (14/0 cm) is characterised by sandy mud with a reduced number of tests (62 tests/15 g), a moderate number of species (8 species, alpha 1.59), and a minimal presence of marine taxa (1%). These values together with dominance of *H. germanica* (39%), *A. tepida* (36%) and *E. oceanense* (17%) suggest more difficult living conditions for these protists under a general brackish environment. Plastic microbeads, together with spherical carbonaceous particles, were also present in this upper unit.

Concentrations of trace metals remain low and fairly constant below 26 cm depth, throughout most of Unit 1 (Fig. 4). Contents of Zn, Pb and Cu in this downcore section (Table 2) are lower than the previously mentioned background levels (Rodríguez et al., 2006). This could be related to the fact that these reference values were calculated on the <63 μm fraction, which usually exhibits enhanced concentrations of trace metals when compared with the <2 mm fraction analysed in this work. Conversely, Cr and Ni are higher, albeit they are within the range of those used to calculate the regional background values (<0.4–71 mg/kg for Cr and 2–57 mg/kg for Ni, see Rodríguez et al., 2006). This local enrichment can be explained by the occurrence of volcanic rocks with high geogenic levels of both elements in the drainage basin of the Urola

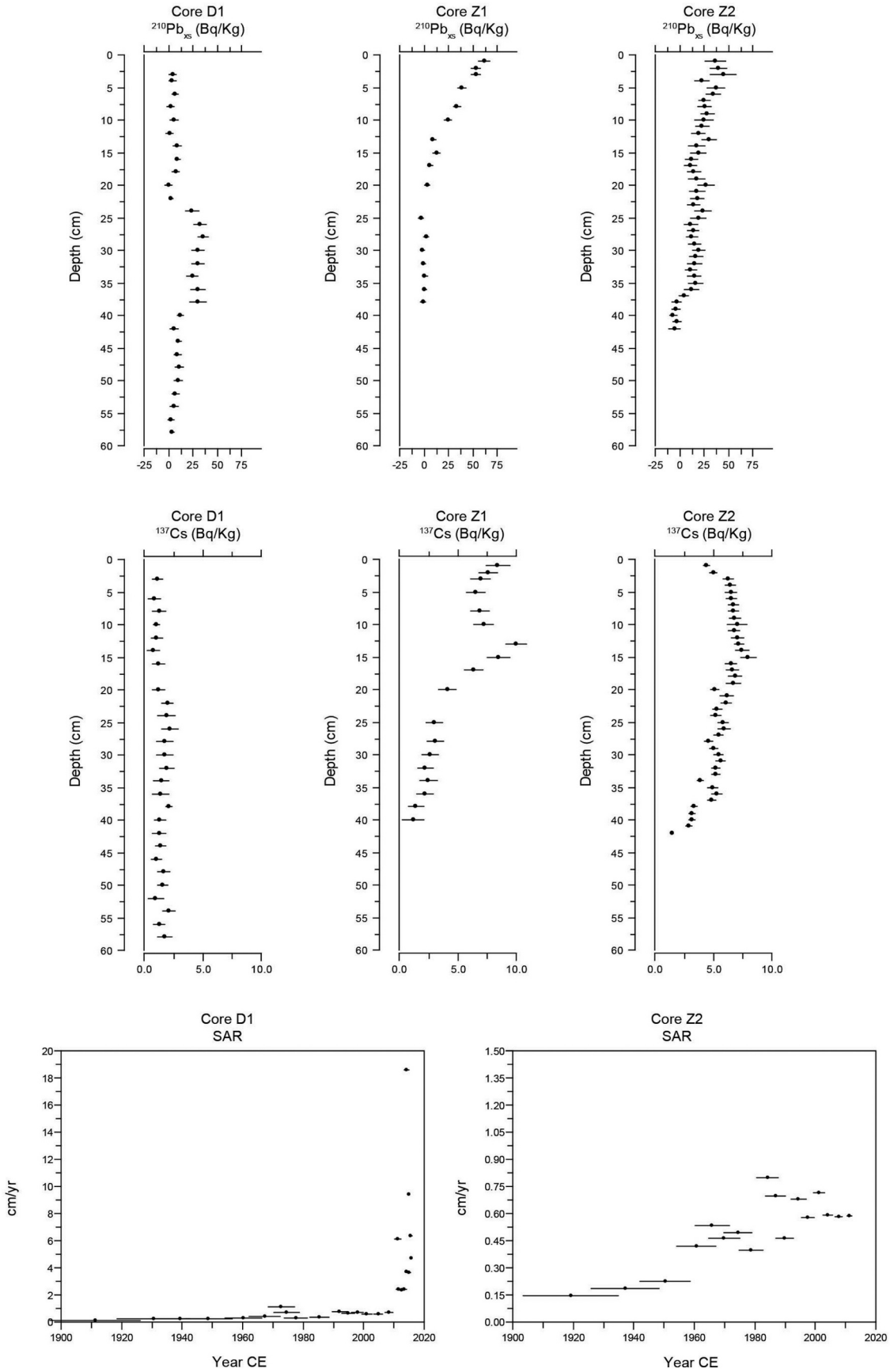

Fig. 5. Distribution of $^{210}Pb_{xs}$ (Bq/kg) and ^{137}Cs (Bq/kg) with depth (cm) in cores D1, Z1 and Z2, and SAR (sediment accumulation rates, cm/yr) through time (yr) in cores D1 and Z2 (Deba and Urola estuaries, Basque Coast Geopark).

Table 3
Summary of microfaunal and geochemical data from surface samples in the Deba and Urola estuaries (Basque Coast Geopark).

	Living assemblages												Dead assemblages											
	Deba estuary								Urola estuary				Deba estuary								Urola estuary			
	1	2	3	4	5	6	7	8	1	2	3	4	1	2	3	4	5	6	7	8	1	2	3	4
E. macrescens %			*	*	*		1		0.3		0.3	1	*	*	62	26	9	*	1		0.5	0.4		0.6
T. inflata %			*	*	*				0.8	0.3		0.7			8	11	7		4	*	0.7	0.2	0.3	0.6
A. tepida %	*	*	*	*	*		78	*	30	18	40	33	*	*		33	45		39	*	32	23	37	34
E. oceanense %			*	*	*		9		20	8	16	22	*	*	9	11	11		48	*	23	9	26	37
C. williamsoni %				*	*		8	*		1	0.5	0.7				4	10		2		1	13	1.3	0.6
H. germanica %		*	*	*	*		4		44	70	39	33	*	*	19	15	19		6	*	36	54	26	19
Standing crop (80 cm^3)	6	2	23	49	87	0	261	12	527	301	654	2620	–	–	–	–	–	–	55	–	90	82	83	79
Similarity Living/Dead %																								
No species	1	2	5	6	7	0	5	3	10	9	11	13	5	4	5	6	6	1	7	8	13	11	22	18
Alpha index	–	–	–	–	–	–	0.92	–	1.91	1.74	2.14	2.75	–	–	1.06	1.06	1.13	–	1.30	–	2.54	2.00	4.49	4.11
Allochthonous %	–	–	–	–	–	–	0	–	0.3	0.6	0.6	2	–	–	0	0	0	–	0	–	0.8	0.4	4.8	2.4
Agglutinated %	–	–	–	–	–	–	1	–	1.4	0.3	0.3	2	–	–	72	37	16	–	5	–	2	0.6	0.5	1.2
Porcellaneous %	–	–	–	–	–	–	0	–	3	2	1	2	–	–	0	0	0	–	0	–	4	0.4	2	4
Hyaline %	–	–	–	–	–	–	99	–	95.6	97.7	98.7	96	–	–	28	63	84	–	95	–	94	99	97.5	94.8
Zn mg/kg	340	444	509	519	461	373	261	359	246	292	465	206												
Pb mg/kg	77	48	68	65	48	46	38	47	60	56	63	50												
Cu mg/kg	70	92	104	83	81	64	52	66	53	53	69	40												
Cr mg/kg	34	75	87	93	70	49	45	58	59	52	52	53												
Ni mg/kg	42	66	74	76	52	55	41	57	41	41	37	38												

* Foraminiferal absolute abundance below 100 individuals/tests.

river (Ihobe, 1998). Therefore, trace metal values in these downcore sediments are likely to represent pre-industrial levels in this area. Conversely, the upper third of Unit 1 exhibits significantly enriched concentrations of Zn, Pb and Cu. The highest values of Zn (827 mg/kg) and Pb (190 mg/kg) appear at 23–22 cm depth, and both metals show a decrease upwards throughout Unit 2. However, even in the topcore sample, they remain higher than those determined at the base of the core. Finally, Cu, Cr and Ni display a different trajectory, increasing to maximum concentrations (120, 80 and 62 mg/kg respectively) at about 10 cm depth before starting to decrease at the near surface samples.

$^{210}Pb_{xs}$ activity decreases exponentially with depth suggesting relatively steady-state accumulation and its concentration is cancelled below 30 cm depth (Fig. 5). The CFCS model was applied to this core to determine the mean sediment accumulation rate, yielding a value of 0.22 ± 0.02 cm/yr. Therefore, lower Unit 1 (below 14 cm depth) was deposited between the beginning of the 20th century and 1954 CE, while the upper Unit 2 represents the following 64 years of sedimentary deposition in the middle estuary. This ^{210}Pb-derived chronology is in agreement with the ^{137}Cs peak (Fig. 5) originating from nuclear weapon testing in the early 1960s, as the highest activitiy of this independent radiotracer appears at 13–12 cm depth (1959–1964 CE).

4.2.3. Core Z2

In this core three different intervals were distinguished (Fig. 4, Table 2). Unit 1 (47/26 cm) is a sandy mud interval containing abundant foraminifera at the base that decrease upwards (average 156 tests/15 g). Hyaline forms *H. germanica* (56%) and *A. tepida* (32%) dominate the assemblage, with *E. oceanense* (5%) as secondary. The number of species is moderate (9 species, alpha 1.74) and the percentage of marine tests is very low (2%). Spherical carbonaceous particles are present abundantly in this basal unit deposited under brackish conditions. The following Unit 2 (26/20 cm) shows scarce foraminifera (15 tests/15 g) indicating hostile environmental conditions for these organisms in this sandy mud interval. Together with spherical carbonaceous particles, iron spheroids were also found here. Finally, Unit 3 (uppermost 20 cm) shows an increasing number of foraminiferal tests to the top of this sandy mud interval (average 166 tests/15 g). The hyaline species *E. oceanense* (35%), *A. tepida* (35%) and *H. germanica* (25%) were the dominant taxa. The percentage of marine tests is very low (1%) and the number of species is moderate (9 species, alpha 1.70) in this assemblage suggesting a brackish environment. In addition to spherical carbonaceous particles and iron spheroids, plastic microbeads were also identified in this upper unit.

The lowest concentrations of metals (128 mg/kg for Zn, and < 35 mg/kg for the rest of the analysed elements) appear in the bottom sample (Fig. 4). They increased rapidly, showing a fairly constant profile along the rest of Unit 1 and Unit 2 (although the content of Cr and Ni are slightly higher in the latter) and a decreasing trend towards more recent sediments in Unit 3. However, values for Zn, Pb, Cu and Cr in the topmost sample (227, 51, 44 and 51 mg/kg respectively) are still higher than those determined at the base of the core and in local pre-industrial sediments (Table 2).

Contrary to that observed in core Z1, concentrations of $^{210}Pb_{xs}$ display an irregular profile that does not fit an ideal exponential curve (Fig. 5). Although excess activities show a decreasing trend in the topcore 15 cm (with some deviations) and below 35 cm depth, no apparent general decline is observed in the interval between 35 and 15 cm depth, suggesting that non-steady-state sediment deposition occurs. This may be related to mixing events (due to physical and/or biological factors) and/or changes in sediment supply, source or energy conditions (Cundy et al., 2003). This sampling site is located less than 200 m upstream from the Balenciaga shipyard, which began to operate in 1921 on the left bank of the estuary and moved to the right bank, just in front of its original location, in the 1940s. This industry requires maintenance dredgings to ensure an adequate navigation channel at depths and widths necessary to allow the departure of the ships. However, some of

the recently deposited sediments removed from the bottom are not captured during dredging operations, and thus significant amounts of suspended particles can be remobilised and redeposited again within the estuary. In fact, dredging has been considered as the main significant anthropogenic pressure (producing negative effects on the environment) detected in this estuary (Tueros et al., 2009). This process of pre-depositional reworking could also contribute to explain the almost constant profiles shown by trace metals (Fig. 4) as well as the vertical distribution of ^{137}Cs (Fig. 5). Even though this radiotracer exhibits a maximum value at 15 cm depth, it does not seem to be related to the 1963 CE peak, as concentrations at the following 19–16 cm depth and the 9–5 cm depth intervals are very similar.

The concentration of $^{210}Pb_{xs}$ is cancelled at 38–37 cm depth (Fig. 5) and the CRS model has been applied in this core to determine the ages and accumulation rates of sediment. Unit 1 has been dated from the final 19th century until 1965 CE, the age calculated for Unit 2 was 1965–1980 CE and Unit 3 was deposited between the years 1980–2015 CE. Similarly to that observed in core D1, sedimentation rates exhibit an increasing trend with time (Fig. 5), since they grew during the 1960s from 0.4 to 0.6 cm/yr, reaching a peak value of 0.8 cm/yr in the mid-1980s.

4.3. Modern surface samples

In all, surface samples of the Deba estuary contained only 339 live foraminifera of 8 different species and 1043 dead tests belonging to 11 taxa (Table 3). In general, live assemblages present a very small number of individuals (minimum standing crop/80 cm^3: 2) and species (1 taxon) in the upper part of the estuary which gradually increase towards the mouth (maximum standing crop/80 cm^3: 261; maximum number of species: 7, alpha 0.92). Regarding dead assemblages, only stations Deba-3, 4, 5 and 7 (middle estuarine area) exceed 100 test/80 cm^3. *Ammonia tepida* is the only dominant species in both the live and dead assemblages, whereas *E. macrescens*, *H. germanica* and *E. oceanense* are the main taxa in the dead assemblages, with *T. inflata* and *C. williamsoni* as secondary species. Agglutinated tests are present abundantly in the dead assemblages (average 33%, range 5–72%). The number of species is low-moderate (between 4 and 8, alpha 1.06–1.30) and marine foraminifera have not been found in these samples. The difference between the number of foraminifera in the live and dead assemblages can be explained by the cumulative nature of the latter over time. This suggests that live foraminifera do not find adequate environmental conditions to reproduce and prevent abundant populations within this estuary. Analysis of the geochemical content of the surface samples shows moderately elevated levels of Pb, Zn, Cu, Ni and Cr in the upper and middle parts of the estuary. The highest concentrations of most trace metals correspond to stations Deba-3 and 4 (Table 3), whereas the lowest values appear in sampling site Deba-7, coinciding with the maximum number of living foraminifera.

Along the Urola estuary, live foraminiferal assemblages are very abundant and dominated by *H. germanica*, which shows greater abundance in the middle zone (44–70%) and decreases moderately towards the mouth (33–39%), *A. tepida* which increases slightly from the middle (18–30%) to the lower reaches (33–40%), and *E. oceanense* that maintains a similar concentration along the estuary (average 17%) (Table 3). In general, live assemblages present a high number of individuals and species which gradually increase towards the lower estuary (standing crop/80 cm^3: 301–2620; number of species: 9–13, alpha 1.74–2.75). Dead assemblages show a similar distribution of the main species and a higher number of taxa (11–22 species, alpha 2.00–4.49) due to its cumulative character and the presence of marine taxa that are more abundant in the lower estuary (0.4–4.8%). The similarity between both assemblages is very high (average 84%), particularly in the middle estuary (82–90%). Trace metals are quite similar to those present in the uppermost samples of the cores, although the high levels of Zn found in the Zumaia-3 station are remarkable (Table 3).

5. Discussion: estuarine evolution at different timescales

Environmental records obtained from the estuaries of the Basque Coast Geopark cover a wide range of temporal scales, ranging from geological (thousands and hundreds of years) to recent times (decades).

5.1. The Deba estuary

During the last 10 ka, the upper-middle Deba estuary infill includes brackish intertidal sediments of muddy and sandy nature, intercalated by fluviatile materials, whereas the lower-middle estuary infill ranges from an older brackish estuarine unit through fluviatile sediments to younger salt marsh deposits. These sedimentary sequences are made up of several metres of fluvial intervals barren of foraminifera. The absence of foraminifera is not considered here as a possible consequence of *post-mortem* test dissolution because calcareous microfossils are very well preserved in sediments from the Basque coast due to the widespread presence of carbonate rocks of Mesozoic-Cenozoic age. This causes fresh water flowing into the estuaries to be saturated in dissolved calcium carbonate and the burial environment to be non-corrosive (Cearreta and Murray, 2000). The resulting preservation of the complete microfossil assemblages is of great advantage for the palaeoenvironmental interpretation of buried sequences. Other features of the Deba estuary geological record include a general presence of coarse sediments, a reduced number of common estuarine taxa, and scarce marine foraminiferal tests. The DEB1 borehole showed a basal muddy and brackish intertidal environment during the initial transformation of the area from a Pleistocene river into a Holocene estuary between >9800 to 9000 yr cal BP. This was followed by a predominantly sandy brackish setting until <6700 yr cal BP, when fluviatile conditions took over up to the human reclamation of the area in the 19th century (Table 1). Common autochthonous foraminiferal species of the Cantabrian estuaries, such as calcareous *A. tepida*, *H. germanica*, *C. williamsoni* and *E. oceanense* (Cearreta and Murray, 1996), dominate the brackish assemblages whereas the fluviatile units are barren of these protists of marine affinity. The most relevant allochthonous species present in the basal unit is *R. irregularis*. The DEB2 borehole started with a sandy and brackish intertidal environment dominated by estuarine foraminiferal taxa deposited between >8800 and 8800 yr cal BP, which was interrupted by near fluviatile conditions with extremely scarce foraminiferal tests during the following 7.7 ka. From <1100 yr cal BP until human reclamation in the 19th century (Rivas and Cendrero, 1992), a salt marsh environment characterised by the typical agglutinated species *T. inflata* and *E. macrescens* was recorded. In coastal areas where regional rocks supply abundant calcium carbonate to the environment, high and low salt marshes can be easily distinguished in the buried sequences, as higher topographic areas are characterised by the exclusive presence of agglutinated foraminiferal species whereas lower zones feature both agglutinated and calcareous forms (Cearreta et al., 2002a; Edwards and Wright, 2015).

Recent materials deposited since the mid-20th century (Anthropocene aged sensu Zalasiewicz et al., 2015) in the Deba estuary are represented by core D1, containing very scarce foraminiferal tests in this middle estuary record. The most representative recent taxa are a mixture of agglutinated *T. inflata* and *E. macrescens*, together with calcareous *A. tepida* and *H. germanica* (Table 2). Fresh-water discharge during recent decades is considered as the main environmental process inhibiting the development of abundant foraminiferal assemblages in this estuary. Even today, modern foraminiferal populations are characterised by extremely low numbers of living individuals along the estuary with only the highly euryhaline taxon *A. tepida* present in sufficient numbers in both the live and dead assemblages (Table 3). Agglutinated species are well represented in the dead assemblages exhibiting a clear decrease towards the lower reaches of the estuary as the calcareous foraminifera increase in abundance. Cumulative dead assemblages are slightly more abundant and diverse containing the same autochthonous

taxa found in the buried assemblages but lacking marine foraminiferal tests. Wang and Murray (1983) correlated foraminiferal assemblages with tidal range and the degree of mixing of fresh and salt water in estuaries, concluding that in river-dominated estuaries marine foraminifera form only a minimal part of the dead assemblage. Consequently, live and dead assemblages are usually similar. Furthermore, Cooper and McMillan (1987) found that hyposaline estuarine channels from South African river-dominated estuaries contain only low diversity *Ammonia*-dominated assemblages. These characteristics are also found in the Deba estuary which reinforces the idea that it has been a fresh-water-dominated environment with minimal marine influence for several millennia. This results in harsh environmental conditions for foraminifera to live and reproduce.

Regarding the geochemical quality of the recent sediments, concentrations of trace metals in surface and cored samples exceed not only the regional background values (Rodríguez et al., 2006) but also those proposed as pre-industrial in the adjacent estuary of Urola (Table 2). This enrichment confirms the historical impact exerted by human activities since at least the late 19th century. The highest metal content corresponds to the mid-1970s (Fig. 4), coinciding with a marked increase in sedimentation rates. Notwithstanding this, only two elements are in excess the Action Level B above which biological effects are expected to occur: Zn (in surface samples from stations Deba-2, 3, 4 and 5, and below 26 cm depth in the D1 core) and Ni (in surface samples from stations Deba-2, 3 and 4, and throughout the entire core). Although local metal coating industries (zinc- and nickel-plating) appear as the most probable anthropogenic source of both metals, it is worth noting that the relatively elevated levels of Ni could be partly related to lithogenic effects, given that the estuaries of Deba and Urola share the same geological setting.

5.2. The Urola estuary

The upper Urola estuary also includes important coarse fluviatile deposits both at the base of the Holocene sequence and again intercalated between older sandy brackish intertidal and younger low salt marsh deposits. However, in the lower estuary the fluvial deposits found above the basement are overlain by a shallowing-upward marine sequence represented by a near-marine sandy intertidal environment below, an intermediate sandy brackish estuarine setting and an uppermost low marsh environment. The presence of abundant gravels and extremely low numbers of allochthonous foraminifera are characteristic features of the upper estuary whereas sandy sediments and foraminiferal assemblages dominanted by marine species are typical of the lower estuarine area. The ZUM1 borehole showed a basal fluvial environment that was older (>11,100–8700 yr cal BP) than the formation of the estuary in the lower Holocene. Then sandy, brackish intertidal conditions that developed between 8700–<6100 yr cal BP were replaced by an almost fluviatile environment during the following 4.9 ka. Finally, a low marsh setting was established between 1200 yr cal BP and the reclamation of the area around the 16th century (Rivas and Cendrero, 1992). Common regional autochthonous species, such as calcareous *H. germanica*, *C. williamsoni*, *A. tepida* and *E. oceanense*, are dominant under brackish intertidal conditions. Agglutinated *T. inflata* and *E. macrescens* together with *A. tepida* are the most abundant low marsh taxa. The absence of foraminifera is characteristic of the fluviatile intervals. In the lower estuary, the ZUM2 borehole exhibited marine intertidal conditions characterised by sandy sediments highly dominated by allochthonous taxa (96%) from >9100 to 8300 yr cal BP. The environment continued to be sandy, but salinity conditions became more brackish as marine taxa halved (51%) during the next millennium and decreased to 7% by 6700 yr cal BP. The most important allochthonous taxa were the robust *C. lobatulus*, *C. rudis* and *E. crispum*. Finally, a low marsh characterised by *T. inflata*, *E. macrescens* and secondary *H. germanica* developed until the reclamation of this area around the 16th century (Table 1).

Environmental conditions during recent decades in Urola are represented by cores Z1 in the middle and Z2 in the lower estuary. In the middle estuary record, marine tests were very scarce. Foraminiferal abundance (*A. tepida*, *H. germanica* and *E. oceanense*) in the lower unit doubled the amount in the upper unit and trace metals (e.g., Cu, Ni and Cr) increased remarkably since the 1960s. In the same way, the lower estuary exhibited a very low presence of allochthonous foraminifera and the autocthonous species *H. germanica*, *A. tepida* and *E. oceanense* almost disappeared during the 1960s, although they recovered after the 1980s when metal concentrations decreased (Table 2). Modern foraminiferal populations are very abundant in this estuary and live and dead assemblages are similar. The same three autochthonous taxa (*H. germanica*, *A. tepida* and *E. oceanense*) dominate both assemblages along the estuary showing a small variation in abundance towards the mouth of the estuary (Table 3).

Different microscopic spheroidal particles were found in recent sediments from the Urola estuary. Firstly, spherical carbonaceous particles appeared in all samples although they were more abundant in the basal Unit 1 of Z1 and Z2 cores. These carbonaceous particles are a distinct form of black carbon produced principally from both coal burning and fuel-oil combustion, and are aerially disseminated. They were first recorded from strata dating to about 1830 CE in the UK and show a near-synchronous global mid-20th century increase in abundance due to large-scale power plants (Rose, 2015; Swindles et al., 2015). In this estuary, these carbonaceous particles would indicate an early human impact as they derive probably from the manufacture of cement, which was the main industrial process developed in the Zumaia area during the second half of the 19th century (the last plant closed in 1972) when the local industry associated with metals had not yet started. It was produced from nearby raw materials, specifically argillaceous limestones, and coal as fuel for calcination. Secondly, iron spheroids were found since the 1960s in the Z2 core (Unit 2). These industrially generated spherules are mainly by-products of solid fuel combustion, iron and steel manufacture and metal smelting (Oldfield, 2014). Finally, plastic microbeads were also present in sediments since the 1980s from the uppermost Unit 2 of the Z1 core and Unit 3 of the Z2 core. They are manufactured particles made of petrochemical plastics and used mainly in cosmetics and personal care products, as well as in various biomedical and industrial applications. They can pass unfiltered through sewage treatment plants and make their way into rivers and estuaries, resulting in plastic particle water pollution (Van Cauwenberghe et al., 2015). Although they have not been quantified in this work, the presence of all these various spheroids in the sediments is considered as a clear indicator of the different industrial activities developed in the Urola estuary in recent times.

In this estuary, Zn is the only trace metal that exceeds the Action Level B for the classification of dredged sediments, in both surface sediments collected in the station Zumaia-3 and cored samples from Z1 (between 25 and 8 cm depth) and Z2 (between 43 and 18 cm depth). These sediments were deposited between the first years of the 20th century and 1978 CE (core Z1) and since the late 19th century until 1983 CE (core Z2). Therefore, although significant pollution is likely to have begun earlier in the lower estuary, the improvement seems to have occurred along the whole estuary sinchronously, starting in the latest 1970s.

5.3. Contrasting estuaries

As registered in their respective geological records, comparison of environmental change at different temporal scales shows important differences between these two adjacent estuaries. On the one side, at millennial and centennial timescales, the Deba estuary can be considered as a river-dominated environment since the lower Holocene until the present. Fluvial coarse deposition (almost) barren of foraminifera took place during the last 8.0 ka, approximately at the boundary between the Greenlandian and the Northgrippian ages located at 8236 yr

cal BP (Walker et al., 2019). This means that fresh-water discharge became the main environmental driver in this estuary during the last eight millennia above other natural processes such as sea-level rise that it is considered worldwide as the main coastal driver during the Holocene Epoch. River-dominated estuaries are unique sedimentary environments associated with high fluvial sediment supply. Many are comparatively short due to the steepness of the hinterland and elevated rainfall promotes high fluvial sediment yields and large fluvial discharge that limits tidal penetration (Cooper, 1993, 2002). All this has important consequences for regional sea-level studies as this geological record indicates a tide-dominated Deba estuary during the Greenlandian Age that evolved into a river-dominated estuary in the Northgrippian Age and has not been governed by marine processes ever since. An estuary may change from one evolutionary mode to another during its geological development, and Cooper (1993) presented evidence of change from tide-dominated to river-dominated conditions over the Holocene timescale in the Mgeni estuary (South Africa). When changes in tidal influence take place, there may be a parallel response in foraminiferal assemblages (Wang and Murray, 1983). Thus, a changing intensity of tidal influence could be recognised as a variation in the foraminiferal abundance in general and in marine foraminiferal tests in particular. This has been the case in the Deba estuary where allochthonous tests are present (average 6–10%) in the basal units of both boreholes and disappeared from the sedimentary record during the following 8.0 ka. A recent sea-level curve for the Basque Country (García-Artola et al., 2018) that comprises sea-level index points from different regional estuaries also includes a few dates from Deba but all of them are older than 8000 yr cal BP and were obtained from the basal brackish units. This temporal boundary marks an important regional sea-level rise rate deceleration from ~6.8 ± 1.2 mm/yr during the previous millennium (9000–8000 yr cal BP) to 3.7 ± 0.5 mm/yr during the following millennium (8000–7000 yr cal BP) with much lower values since then until the present (García-Artola et al., 2018). On the contrary, the Urola estuary contains a Holocene geological record dominated by the interplay between fluvial and marine processes in the upper estuary and by marine processes only in the lower estuary. Here deposition of different sandy and muddy units was characterised by a decreasing salinity and marine influence during the last 9.0 ka as regional sea-level rise rate diminished from 8.4 ± 1.5 mm/yr during the interval 10,000–9000 yr cal BP to 0.7 ± 1.6 mm/yr in the last millennium. This implies that Urola has been a tide-dominated estuary since its formation despite the important decelerations in regional sea-level rise that have taken place.

On the other side, at decadal timescale, since the late 19th century to the present, the recent sediments from Deba contain a greater concentration of industrial trace metals and a much lower number of benthic foraminifera than the Urola estuary. These could be interpreted as indicative of a greater industrial impact on these organisms in the former estuary. However, the millennial environmental evolution of the estuary shows that this industrial impact on the recent benthic foraminiferal assemblages seems to be negligible as populations of these protists have been naturally very scarce due to fresh-water-dominant conditions in this estuary. On the contrary, the recent record from the Urola estuary, with lower metal content and higher numbers of foraminifera, shows impacted foraminiferal assemblages during the interval 1960–1980s. During those decades, anthropogenic trace metals do not show a significant episode of increase but foraminifera halved in the middle estuary and almost disappeared in the lower estuary where most anthropogenic activities were concentrated, in contrast with their greater and similar abundances both before and after this time interval. In the Basque coastal area, despite recently increased trace metal concentrations, the occurrence of foraminiferal assemblages in young industrial sediments and along modern estuaries has not been related to defined levels of trace metals (Cearreta et al., 2002b). Similarly, the most abundant recent forms in these estuaries, *A. tepida* and *H. germanica*, have demonstrated great tolerance to trace metals and different contaminants in other polluted and industrial coastal sites (Samir and El-Din, 2001; Bergamin et al., 2003; Denoyelle et al., 2012). However, remobilization of sediments resulting from dredging activities can be responsible for the deterioration of the estuarine sediment quality. These activities resuspend fine materials into the water column and can render pollutants to be bioavailable to biota (Nayar et al., 2003) and cause intense oxygen depletion in the estuary (Leorri et al., 2008). They can be reflected in the reduction of the total number of individuals and taxa of benthic organisms (Newell et al., 1998; Cruz-Motta and Collins, 2004). In the fine deposits that characterise coastal ecosystems, Newell et al. (1998) reported that recolonisation can take several years in areas of low current velocity. High concentrations of contaminants related to dredging activities in the Urola estuary were found previously by Solaun et al. (2015) and a dramatic reduction in both the foraminiferal abundance and diversity due to dredging has been encountered in various estuaries by Ruiz et al. (2004), Leorri et al. (2008), Jayaraju et al. (2010) and Mojtahid et al. (2016).

Regarding metal contamination, sediments from both estuaries exhibit a significantly high content of Zn (above the Action Level B), confirming the role of this element as one of the most widespread chemicals in the coastal environments of the Basque Country (Irabien et al., 2018, 2020a, 2020b). Although concentrations are not high enough to preclude unconfined, open water disposal, if these sediments had to be remobilised it would be highly recommended to perform toxicity analyses to find the best management alternative. Given that the anomalous Zn content appears not only in some surface samples, but also in layers "hidden" beneath a mantle of cleaner sediments, obtained results underpin the need to address the study of recent sedimentary deposits from an integral perspective that includes their historical development. Moreover, this approach allows assessing the evolution of sediment accumulation rates, which is usually used as an indicator of the intensity of the geomorphic processes. Two of the three studied cores have recorded an increase in this parameter, particularly since the 1960s (Fig. 5). This is in good agreement with the acceleration observed by Bruschi et al. (2012) in eight estuaries of the northern Spanish coast, most probably due to human-induced geomorphic change rather than climate change (also human-induced). Anthropogenic mixing or anthroturbation in aquatic areas refers to the disturbance of sediments by human intervention such as construction, bottom trawling, dredging, dumping, trenching, anchoring and even sediment sampling (Soulsby et al., 2007; Bunke et al., 2019). These activities, by themselves, usually exert a direct effect on the areas where they are developed. However, our results indicate that they likely have an indirect impact on the surrounding areas through the redeposition of reworked materials, derived from the public works executed around the Deba estuary and due to maintenance dredgings in Urola.

River-dominated estuaries, where tidal flow is low relative to the fluvial discharge, are associated with high fine-sediment supply transported in suspension and discharged seaward of the river mouth into the continental shelf where they can present offshore mud depocentres (Cooper, 2002). These fine-grained depocentres can document the environmental dynamics of the source estuaries through time and play a role in the biogeochemical cycle of derived trace metals and other pollutants (Horne and Patton, 1989; Dzwonkowski et al., 2015; Wang et al., 2018). This is the case of the Basque Mud Patch, located in front of the Basque Coast Geopark, where Irabien et al. (2020a) found concentrations of metals reflecting an increasing trend of anthropogenic activities since the late 19th century related to the industrialization of the nearby estuaries, including the turbid Deba estuary.

6. Conclusion

The Deba and Urola are the only estuaries in the Basque Coast Geopark otherwise characterised by a rocky coast made of steep cliffs. Despite their proximity, they have exhibited very different environmental conditions through time. The Deba estuary changed from a tide-dominated to a river-dominated environment in the lower Holocene,

and fresh-water discharge became its main environmental driver during the last eight millennia. Consequently, today it is one of the most turbid estuaries on the southern Bay of Biscay. On the contrary, the Urola estuary exhibits a Holocene geological record dominated by marine processes in response to a decreasing regional sea-level rise rate during the last 9.0 ka. It has been a tide-dominated setting since its formation and it represents one of the least turbid estuaries on this coastal area.

The concentration of trace metals in recent and modern sediments is regarded worldwide as one of the main signatures of anthropogenic impact on the estuaries. Although sediments deposited in these Basque estuaries are enriched in trace metals due to urban and industrial effluents discharged for decades, their impact on the foraminiferal populations has been negligible. In Deba, these protists of saline affinity are naturally very scarce due to enduring fresh-water-dominant conditions in this estuary. In Urola, its abundant foraminiferal assemblages have been impacted more severely by the intense dredging operations performed historically in the lower estuary. As sediments from both estuaries store high amounts of Zn, in case of remobilization of these materials by public works or maintenance dredgings, it is recommended to perform toxicity analyses to warrant correct decision on the most adequate management option.

This work demonstrates that assessment of the natural conditions and anthropogenic impacts in an estuarine domain is a complex task that should require knowledge of its original environmental features, including their spatial and temporal variability, as registered in its Quaternary geological record.

Funding

This research was supported financially by Geoparkea-UPV/EHU (US13/02), Spanish MINECO (CGL2013-41083-P and RTI2018-095678-B-C21, MCIU/AEI/FEDER, UE), UPV/EHU (UFI11/09) and EJ/GV (IT365-10, IT767-13 and IT976-16) projects. NEA is supported by the Centre for Arctic Gas Hydrate, Environment and Climate (CAGE), the Research Council of Norway through its Centres of Excellence scheme (grant 223259). These funding sources were not involved in the study design, the collection, analysis and interpretation of data, the writing of the report, or the decision to submit the article for publication.

Declaration of Competing Interest

None.

Acknowledgements

Dr. Asier Hilario (Scientific Director of the Basque Coast Geopark) supplied the necessary administrative authorizations and greatly supported this work. Core D1 was retrieved by the Geology Group of the University of Cantabria (Drs. Juan Remondo, Jaime Bonachea and Mario Morellón). José Gaminde (Aroa Geotecnia SLL) was responsible for the drilling activities. Microfossil samples of boreholes DEB1, ZUM1 and ZUM2, and core D1 were prepared and analysed initially by Sergio Hernández-Martín, Ziortza García-Fernández and Khalid Soualili. SEM-EDX analyses were performed at the Electronic Microscopy and Material Microanalysis Service (SGIker, UPV/EHU/ERDT, EU). José Agustín Egiguren and Iñaki Egaña (Deba city council) facilitated drilling operations in their municipality. Two anonymous reviewers improved the original manuscript with their comments and suggestions. It is contribution 52 of the Geo-Q Zentroa Research Unit (Joaquín Gómez de Llarena Laboratory).

Appendix A

Table A1
Reference list of autochthonous (E, estuarine) and allochthonous (M, marine) foraminiferal species found in the Deba and Urola estuaries (Basque Coast Geopark) grouped by wall type.

Estuarine (Authochthonous)
Agglutinated Test
Arenoparrella mexicana (Kornfeld) = *Trochammina inflata* var. *mexicana* Kornfeld, 1931
Cribrostomoides jeffreysii (Williamson) = *Nonionina jeffreysii* Williamson, 1858
Entzia macrescens (Brady) = *Trochammina inflata* (Montagu) var. *macrescens* Brady, 1870
Lepidodeuterammina ochracea (Williamson) = *Rotalina ochracea* Williamson, 1858
Miliammina fusca (Brady) = *Quinqueloculina fusca* Brady, 1870
Tiphotrocha comprimata (Cushman & Brönnimann) = *Trochammina comprimata* Cushman & Brönnimann, 1948
Trochammina inflata (Montagu) = *Nautilus inflatus* Montagu, 1808

Porcellaneous Test
Cornuspira involvens (Reuss) = *Operculina involvens* Reuss, 1850
Quinqueloculina jugosa Cushman, 1944
Quinqueloculina seminula (Linnaeus) = *Serpula seminulum* Linnaeus, 1758

Hyaline Test
Ammonia tepida (Cushman) = *Rotalia beccarii* var. *tepida* Cushman, 1926
Aubignyna hamblensis Murray, Whittaker & Alve, 2000
Bolivina pseudoplicata Heron-Allen & Earland, 1930
Bolivina britannica Macfadyen, 1942
Cribroelphidium excavatum (Terquem) = *Polystomella excavata* Terquem, 1875
Cribroelphidium williamsoni (Haynes) = *Elphidium williamsoni* Haynes, 1973
Elphidium margaritaceum Cushman, 1930
Elphidium oceanense (d'Orbigny in Fornasini) = *Polystomella oceanensis* d'Orbigny, 1826
Fissurina lucida (Williamson) = *Entosolenia marginata* var. *lucida* Williamson, 1848
Haynesina germanica (Ehrenberg) = *Nonionina germanica* Ehrenberg, 1840

Marine (Allochthonous)
Agglutinated Test
Connemarella rudis (Wright) = *Gaudryina rudis* Wright, 1900
Haplophragmoides wilberti Andersen, 1953
Spiroplectinella wrightii (Silvestri) = *Spiroplecta wrightii* Silvestri, 1903
Textularia sagittula Defrance, 1824

(*continued on next page*)

Table A1 (*continued*)

Estuarine (Authochthonous)
Textularia truncata Höglund, 1947

Porcellaneous Test
Adelosina bicornis (Walker & Jacob) = *Serpula bicornis* Adams, 1798
Adelosina ferussacii (d'Orbigny, sp. Brady) = *Miliolina ferussacii* d'Orbigny, sp. Brady, 1884
Adelosina longirostra (d'Orbigny) = *Quinqueloculina longirostra* d'Orbigny, 1826
Adelosina striata d'Orbigny, 1826
Massilina secans (d'Orbigny) = *Quinqueloculina secans* d'Orbigny, 1826
Miliolinella subrotunda (Montagu) = *Vermiculum subrotundum* Montagu, 1803
Quinqueloculina lata Terquem, 1876
Quinqueloculina sp.
Siphonaperta quadrata (Nørvang) = *Quinqueloculina quadrata* Nørvang, 1945
Spiroloculina sp.
Triloculina bermudezi Acosta, 1940
Triloculina oblonga (Montagu) = *Vermiculum oblongum* Montagu, 1803
Triloculina trigonula (Lamarck) = *Miliolites trigonula* Lamarck, 1804

Hyaline Test
Acervulina inhaerens Schulze, 1854
Acervulina sp.
Asterigerinata mamilla (Williamson) = *Rotalina mamilla* Williamson, 1858
Bolivina difformis (Williamson) = *Textularia variabilis* var. *difformis* Williamson, 1858
Bolivina spathulata (Williamson) = *Textularia variabilis* var. *spathulata* Williamson, 1858
Bolivina variabilis (Williamson) = *Textularia variabilis* Williamson, 1858
Bulimina elongata d'Orbigny, 1846
Bulimina gibba Fornasini, 1902
Cassidulina obtusa Williamson, 1858
Cibicidoides lobatulus (Walker & Jacob) = *Nautilus lobatulus* Walker y Jacob, 1798
Cribroelphidium gerthi (van Voorthuysen) = *Elphidium gerthi* van Voorthuysen, 1957
Cribroelphidium selseyense (Heron-Allen & Earland) = *Polystomella striatopunctata* var. *selseyensis* Heron-Allen & Earland, 1911
Elphidium crispum (Linnaeus) = *Nautilus crispus* Linnaeus, 1758
Elphidium macellum (Fichtel & Moll) = *Nautilus macellum* Fichtel & Moll, 1798
Favulina hexagona (Williamson) = *Entosolenia squamosa* var. *hexagona* Williamson, 1848
Fissurina marginata (Montagu) = *Vermiculum marginatum* Montagu, 1803
Fissurina orbignyana Seguenza, 1862
Fissurina sp.
Gavelinopsis praegeri (Heron-Allen & Earland) = *Discorbina praegeri* Heron-Allen & Earland, 1913
Globulina gibba (d'Orbigny in Deshayes) = *Polymorphina gibba* d'Orbigny in Deshayes, 1832
Haynesina depressula (Walker & Jacob) = *Nautilus depressulus* Walker & Jacob, 1798
Homalohedra williamsoni (Alcock) = *Entosolenia williamsoni* Alcock, 1865
Lagena semistriata Williamson, 1848
Lagena sulcata (Walker & Jacob) = *Serpula sulcata* Adams, 1798
Lagena sp.
Lamarckina haliotidea (Heron-Allen & Earland) = *Pulvinulina haliotidea* Heron-Allen & Earland, 1911
Planorbulina mediterranensis d'Orbigny, 1826
Pseudononion japonicum Asano, 1936
Pseudononion sp.
Rosalina anomala Terquem, 1875
Rosalina globularis d'Orbigny, 1826
Rosalina irregularis (Rhumbler) = *Discorbina irregularis* Rhumbler, 1906
Stainforthia fusiformis (Williamson) = *Bulimina pupoides* var. *fusiformis* Williamson, 1858
Svratkina sp.
Trifarina angulosa (Williamson) = *Uvigerina angulosa* Williamson, 1858
Uvigerina peregrina Cushman, 1923

Table A2
Radiocarbon dates from boreholes drilled in the Deba and Urola estuaries (Basque Coast Geopark).

Core/Elevation (m LOD)	Lab. number	Material	Method	Conventional ^{14}C age BP	$^{13}C/^{12}C$ ratio (‰)	2σ calibrated age (cal BP)	Median probability
DEB1 (−1.97)	Beta-257958	peat	AMS	5920 ± 40	−27.7	6804–6655 6852–6810	6741
DEB1 (−3.97)	Beta-257959	peat	AMS	6600 ± 50	−29.3	7523–7427 7570–7527	7493
DEB1 (−5.67)	Beta-257960	peat	AMS	6130 ± 50	−26.8	6865–6863 7163–6884	7019
DEB1 (−10.97)	Beta-257961	organic sediment	AMS	9840 ± 60	−26.7	11,401–11,163 11,462–11,453 11,595–11,589	11,251
DEB1 (−12.77)	Beta-257962	organic sediment	AMS	12,190 ± 70	−24.9	13,836–13,811 13,947–13,846 14,329–13,973 14,779–14,732	14,106

(*continued on next page*)

Table A2 (*continued*)

Core/Elevation (m LOD)	Lab. number	Material	Method	Conventional ^{14}C age BP	^{13}C/^{12}C ratio (‰)	2σ calibrated age (cal BP)	Median probability
DEB1 (−14.72)	Beta-257963	peat	AMS	7970 ± 50	−27.3	8681–8645 8994–8686	8835
DEB1 (−16.97)	Beta-257964	peat	AMS	8170 ± 50	−28.9	9275–9007	9115
DEB1 (−17.57)	Beta-257965	shell	AMS	8370 ± 50	−2.0	9080–8590	8846
DEB1 (−19.37)	Beta-257966	peat	AMS	8330 ± 60	−28.9	9185–9134 9478–9192	9342
DEB1 (−19.75)	Beta-257967	peat	AMS	8410 ± 60	−29.4	9533–9289	9436
DEB1 (−22.37)	Beta-257968	peat	AMS	8740 ± 60	−29.3	9913–9543 10,113–10,070	9725
DEB1 (−22.75)	Beta-257969	peat	radiometric	8870 ± 80	−28.1	10,206–9681	9967
DEB1 (−23.16)	Beta-257970	peat	AMS	8790 ± 60	−29.3	9584–9555 9963–9588 10,014–9987 10,043–10,020 10,132–10,060 10,141–10,139	9818
DEB2 (−3.20)	Beta-410167	wood	AMS	1200 ± 30	−25.9	1022–1006 1177–1057 1220–1213 1244–1223	1119
DEB2 (−3.80)	Beta-410168	wood	AMS	1100 ± 30	−25.4	945–933 1063–955	1002
DEB2 (−14.00)	Beta-410169	shell	AMS	8360 ± 30	−0.3	9028–8592	8835
DEB2 (−14.90)	Beta-410170	shell	AMS	8070 ± 30	−1.8	8647–8280	8460
DEB2 (−15.80)	Beta-410171	shell	AMS	8360 ± 30	+1.8	9028–8592	8835
DEB2 (−16.70)	Beta-410172	shell	AMS	8320 ± 30	−0.9	8993–8568	8784
ZUM1 (−2.69)	Beta-433847	wood	AMS	1260 ± 30	−28.9	1096–1076 1163–1120 1282–1175	1217
ZUM1 (−7.19)	Beta-433848	shell	AMS	5870 ± 30	−5.5	6360–5980	6179
ZUM1 (−8.09)	Beta-433849	shell	AMS	5320 ± 30	−3.4	5784–5384	5584
ZUM1 (−9.89)	Beta-433850	wood	AMS	7140 ± 30	−27.4	7890–7875 8015–7931	7964
ZUM1 (−10.79)	Beta-433851	shell	AMS	7720 ± 30	−4.4	8209–7924	8088
ZUM1 (−11.69)	Beta-433852	shell	AMS	7500 ± 30	+0.1	8016–7680	7860
ZUM1 (−12.59)	Beta-433853	wood	AMS	7480 ± 30	−27.2	8269–8195 8371–8279	8293
ZUM1 (−13.49)	Beta-433854	shell	AMS	8030 ± 30	+1.0	8592–8231	8417
ZUM1 (−14.39)	Beta-433855	shell	AMS	8320 ± 30	−5.7	8993–8568	8784
ZUM1 (−16.19)	Beta-433856	plant material	AMS	7900 ± 30	−29.1	8781–8596 8862–8831 8893–8883 8976–8917	8703
ZUM1 (−18.89)	Beta-433857	shell	AMS	10,090 ± 30	−7.2	11,309–10,867	11,124
ZUM2 (−2.84)	Beta-433833	wood	AMS	5910 ± 30	−30.8	6795–6661 6826–6824	6726
ZUM2 (−3.74)	Beta-433834	wood	AMS	6030 ± 30	−26.2	6757–6754 6956–6785	6873
ZUM2 (−4.64)	Beta-433835	wood	AMS	5950 ± 30	−27.1	6854–6675 6880–6873	6774
ZUM2 (−5.24)	Beta-433836	shell	AMS	7030 ± 30	−1.0	7570–7256	7419
ZUM2 (−5.84)	Beta-433837	shell	AMS	6920 ± 30	−0.1	7479–7151	7319
ZUM2 (−6.44)	Beta-433838	shell	AMS	7580 ± 30	−1.4	8135–7768	7942
ZUM2 (−7.34)	Beta-433839	shell	AMS	7050 ± 30	−6.4	7585–7269	7438
ZUM2 (−8.24)	Beta-433840	shell	AMS	7250 ± 30	+2.1	7786–7451	7617

(*continued on next page*)

Table A2 (*continued*)

Core/Elevation (m LOD)	Lab. number	Material	Method	Conventional ^{14}C age BP	^{13}C/^{12}C ratio (‰)	2σ calibrated age (cal BP)	Median probability
ZUM2 (−9.14)	Beta-433841	shell	AMS	6670 ± 30	−3.8	7252–6866	7063
ZUM2 (−10.04)	Beta-433842	shell	AMS	7710 ± 30	−0.3	8274–7915	8078
ZUM2 (−10.94)	Beta-433843	wood	AMS	7440 ± 30	−27.9	8340–8186	8265
ZUM2 (−11.84)	Beta-433844	shell	AMS	7960 ± 30	−0.1	8519–8167	8340
ZUM2 (−13.64)	Beta-433845	shell	AMS	7880 ± 30	−0.7	8413–8060	8256
ZUM2 (−16.34)	Beta-433846	shell	AMS	8540 ± 30	−0.5	9301–8870	9087

LOD: local ordnance datum.

References

Aldabaldetrecu, P., 1993. Estuario del Deba. Deba negua 93, 37–47.

Álvarez-Iglesias, P., Quintana, B., Rubio, B., Pérez-Arlucea, M., 2007. Sedimentation rates and trace metal history in intertidal sediments from San Simon Bay (Ria de Vigo, NW Spain) derived from ^{210}Pb and ^{137}Cs chronology. J. Environ. Radioact. 98, 229–250. https://doi.org/10.1016/j.jenvrad.2007.05.001.

Appleby, P.G., Oldfield, F., 1978. The calculation of ^{210}Pb dates assuming a constant rate of supply of unsupported ^{210}Pb to the sediment. Catena 5, 1–8. https://doi.org/10.1016/S0341-8162(78)80002-2.

Appleby, P.G., Oldfield, F., 1983. The assessment of ^{210}Pb data from sites with varying sediment accumulation rates. Hydrobiologia 103, 29–35. https://doi.org/10.1007/BF00028424.

Appleby, P.G., Oldfield, F., 1992. Applications of ^{210}Pb to sedimentation studies. In: Ivanovich, M., Harmon, R.S. (Eds.), Uranium-Series Disequilibrium. Applications to Earth, Marine and Environmental Sciences, 2nd ed. Oxford Science, Oxford, pp. 731–778.

AZTI, 2020. Red de seguimiento del estado ecológico de las aguas de transición y costeras de la Comunidad Autónoma del País Vasco. Informe de resultados, Campaña (410 pp.).

Baceta, J.I., Orue-Etxebarria, X., Apellaniz, E., 2010. El flysch entre Deba y Zumaia. Enseñ. Cienc. Tier. 18, 269–283.

Baptista Neto, J.A., Ferreira Barreto, C., Guterres Vilela, C., Monteiro da Fonseca, E., Vaz Melo, G., Monica Barth, O., 2017. Environmental change in Guanabara Bay, SE Brazil, based in microfaunal, pollen and geochemical proxies in sedimentary cores. Ocean Coast. Manag. 143, 4–15. https://doi.org/10.1016/j.ocecoaman.2016.04.010.

Belzunce, M.J., Solaun, O., Valencia, V., Pérez, V., 2004a. Contaminants in estuarine and coastal waters. In: Borja, A., Collins, M. (Eds.), Oceanography and Marine Environment of the Basque Country, Elsevier Oceanography Series, vol. 70, pp. 233–251. https://doi.org/10.1016/S0422-9894(04)80047-3.

Belzunce, M.J., Solaun, O., González Oreja, J.A., Millán, E., Pérez, V., 2004b. Contaminants in sediments. In: Borja, A., Collins, M. (Eds.), Oceanography and Marine Environment of the Basque Country, Elsevier Oceanography Series, vol. 70, pp. 283–315. https://doi.org/10.1016/S0422-9894(04)80050-3.

Benito Domínguez, A.M., 2012. Los puertos de Gipuzkoa y sus proyectos. Itsas Memoria: Rev. Estud. Marít. País Vasco 7, 11–50.

Bergamin, I., Romano, E., Gabellini, M., Ausili, A., Carboni, M.G., 2003. Chemical-physical and ecological characterisation in the environmental project of a polluted coastal area: the Bagnoli case study. Mediterr. Mar. Sci. 4, 5–20. https://doi.org/10.12681/mms.225.

Blaauw, M., 2010. Methods and code for "classical" age-modelling of radiocarbon sequences. Quat. Geochronol. 5, 512–518. https://doi.org/10.1016/j.quageo.2010.01.002.

Borja, A., Solaun, O., Franco, J., Pérez, V., 2004. Biomonitoring of heavy metals and organic compounds, at the tissueorganism level. In: Borja, A., Collins, M. (Eds.), Oceanography and Marine Environment of the Basque Country, Elsevier Oceanography Series, vol. 70, pp. 319–333. https://doi.org/10.1016/S0422-9894(04)80051-5.

Borja, A., Galparsoro, I., Solaun, O., Muxika, I., Tello, E.M., Uriarte, A., Valencia, V., 2006. The European Water Framework Directive and the DPSIR, a methodological approach to assess the risk of failing to achieve good ecological status. Estuar. Coast. Shelf S. 66, 84–96. https://doi.org/10.1016/j.ecss.2005.07.021.

Borja, A., Chust, G., Rodríguez, J.G., Bald, J., Belzunce-Segarra, M.J., Franco, J., Garmendia, J.M., Larreta, J., Menchaca, I., Muxika, I., Solaun, O., Revilla, M., Uriarte, A., Valencia, V., Zorita, I., 2016. "The past is the future of the present": learning from long-time series of marine monitoring. Sci. Total Environ. 566–567, 698–711. https://doi.org/10.1016/j.scitotenv.2016.05.111.

Bruschi, V.M., Bonachea, J., Remondo, J., Gómez-Arozamena, J., Rivas, V., Méndez, G., Naredo, J.M., Cendrero, A., 2012. Analysis of geomorphic systems' response to natural and human drivers in northern Spain: implications for global geomorphic change. Geomorphology 196, 267–279. https://doi.org/10.1016/j.geomorph.2012.03.017.

Buceta, J.L., Lloret, A., Antequera, M., Obispo, R., Sierra, J., Martínez-Gil, M., 2015. Nuevo marco para la caracterización y clasificación del material dragado en España. Ribagua 2, 105–115. https://doi.org/10.1016/j.riba.2015.11.001.

Bunke, D., Leipe, T., Moros, M., Morys, C., Tauber, F., Virtasalo, J.J., Forster, S., Arz, H. W., 2019. Natural and anthropogenic sediment mixing processess in the South-Western Baltic Sea. Front. Mar. Sci. 6, 677. https://doi.org/10.3389/fmars.2019.00677.

Cearreta, A., 1988. Distribution and ecology of benthic foraminifera in the Santoña estuary, Spain. Rev. Esp. Paleontol. 3, 23–38.

Cearreta, A., Murray, J.W., 1996. Holocene paleoenvironmental and relative sea-level changes in the Santoña estuary, Spain. J. Foramin. Res. 26, 289–299. https://doi.org/10.2113/gsjfr.26.4.289.

Cearreta, A., Murray, J.W., 2000. AMS ^{14}C dating of Holocene estuarine deposits: consequences of high-energy and reworked foraminífera. Holocene 10, 155–159. https://doi.org/10.1191/095968300669405262.

Cearreta, A., Irabien, M.J., Ulibarri, I., Yusta, I., Croudace, I.W., Cundy, A.B., 2002a. Recent salt marsh development and natural regeneration of reclaimed areas in the Plentzia Estuary, N. Spain. Estuar. Coast. Shelf S. 54, 863–886. https://doi.org/10.1006/ecss.2001.0862.

Cearreta, A., Irabien, M.J., Leorri, E., Yusta, I., Quintanilla, A., Zabaleta, A., 2002b. Environmental transformation of the Bilbao estuary, N. Spain: microfaunal and geochemical proxies in the recent sedimentary record. Mar. Pollut. Bull. 44, 487–503. https://doi.org/10.1016/S0025-326X(01)00261-2.

Cearreta, A., Irabien, M.J., Pascual, A., 2004. Human activities along the Basque coast during the last two centuries: geological perspective of recent anthropogenic impact on the coast and its environmental consequences. In: Borja, A., Collins, M. (Eds.), Oceanography and Marine Environment of the Basque Country, Elsevier Oceanography Series, vol. 70, pp. 27–50. https://doi.org/10.1016/S0422-9894(04)80040-0.

Cearreta, A., García-Artola, A., Leorri, E., Irabien, M.J., Masque, P., 2013. Recent environmental evolution of regenerated salt marshes in the southern Bay of Biscay: anthropogenic evidences in their sedimentary record. J. Mar. Syst. 109–110, S203–S212. https://doi.org/10.1016/j.jmarsys.2011.07.013.

Cheng, J., Collins, L.S., Holmes, C., 2012. Four thousand years of habitat change in Florida Bay, as indicated by benthic foraminifera. J. Foraminifer. Res. 42, 3–17. https://doi.org/10.2113/gsjfr.42.1.3.

Chust, G., Borja, A., Liria, P., Galparsoro, I., Marcos, M., Caballero, A., Castro, R., 2009. Human impacts overwhelm the effects of sea-level rise on Basque coastal habitats (N Spain) between 1954 and 2004. Estuar. Coast. Shelf S. 84, 453–462. https://doi.org/10.1016/j.ecss.2009.07.010.

Comisión Interministerial de Estrategias Marinas, 2015. Directrices para la caracterización del material dragado y para su reubicación en aguas del dominio público marítimo-terrestre (61 pp.).

Cooper, J.A.G., 1993. Sedimentation in a river dominated estuary. Sedimentology 40, 979–1017. https://doi.org/10.1111/j.1365-3091.1993.tb01372.x.

Cooper, J.A.G., 2002. The role of extreme floods in estuary-coastal behaviour: contrasts between river- and tide-dominated microtidal estuaries. Sediment. Geol. 150, 123–137. https://doi.org/10.1016/S0037-0738(01)00271-8.

Cooper, J.A.G., McMillan, I.K., 1987. Foraminifera of the Mgeni Estuary, Durban, and their sedimentological significance. S. Afr. J. Geol. 90, 489–498.

Costanza, R., d'Arge, R., de Groot, R., Farber, S., Grasso, M., Hannon, B., Limburg, K., Naeem, S., O'Neill, R.V., Paruelo, J., Raskin, R.G., Sutton, P., van den Belt, M., 1997. The value of the world's ecosystem services and natural capital. Nature 387, 253–260. https://doi.org/10.1038/387253a0.

Cruz-Motta, J.J., Collins, J., 2004. Impacts of dredged material disposal on a tropical soft-bottom benthic assemblage. Mar. Pollut. Bull. 48, 270–280. https://doi.org/10.1016/j.marpolbul.2003.08.002.

Cundy, A.B., Croudace, I.W., Cearreta, A., Irabien, M.J., 2003. Reconstructing historical trends in metal-input in heavily-disturbed, contaminated estuaries: studies from Bilbao, Southampton Water and Sicily. J. Appl. Geochem. 18, 311–325. https://doi.org/10.1016/S0883-2927(02)00127-0.

Debenay, J.P., Guillou, J.-J., Redois, F., Geslin, E., 2000. Distribution trends of foraminiferal assemblages in paralic environments: a base for using foraminifera as

bioindicators. In: Donald, E., Kluver, M. (Eds.), Environmental Micropaleontology. Springer, Berlin, pp. 39–67.
Denoyelle, M., Geslin, E., Jorissen, F.J., Cazes, L., Galgani, F., 2012. Innovative use of foraminifera in ecotoxicology: a marine chronic bioassay for testing potential toxicity of drilling muds. Ecol. Indic. 12, 17–25. https://doi.org/10.1016/j.ecolind.2011.05.011.
Dzwonkowski, B., Park, K., Collini, R., 2015. The coupled estuarine-shelf response of a river-dominated system during the transition from low to high discharge. J. Geophys. Res. Oceans 120, 6145–6163. https://doi.org/10.1002/2015JC010714.
Edwards, R., Wright, A., 2015. Foraminifera. In: Shennan, I., Long, A.J., Horton, B.P. (Eds.), Handbook of Sea-Level Research. John Wiley & Sons, Chichester, pp. 191–217.
El bani Altuna, N., Cearreta, A., Irabien, M.J., Gómez Arozamena, J., Hernández, S., Soualili, K., Hilario, A., 2019. Evolución ambiental del estuario del Deba (Geoparque de la Costa Vasca) durante el Holoceno y el Antropoceno. Geogaceta 66, 63–66.
Fisher, R.A., Corbett, A.S., Williams, C.B., 1943. The relationship between the number of species and the number of individuals in a random sample of an animal population. J. Anim. Ecol. 12, 42–58.
Franco, J., Borja, A., Valencia, V., 2004. Overall assessment - human impacts and quality status. In: Borja, A., Collins, M. (Eds.), Oceanography and Marine Environment of the Basque Country, Elsevier Oceanography Series, vol. 70, pp. 581–597. https://doi.org/10.1016/S0422-9894(04)80061-8.
García-Artola, A., Cearreta, A., Irabien, M.J., Leorri, E., Sanchez-Cabeza, J.A., Corbett, D. R., 2016. Agricultural fingerprints in salt-marsh sediments and adaptation to sea-level rise in the eastern Cantabrian coast (N. Spain). Estuar. Coast. Shelf S. 171, 66–76. https://doi.org/10.1016/j.ecss.2016.01.031.
García-Artola, A., Stéphan, P., Cearreta, A., Kopp, R.E., Khan, N.S., Horton, B.P., 2018. Holocene sea-level database from the Atlantic coast of Europe. Quat. Sci. Rev. 196, 177–192. https://doi.org/10.1016/j.quascirev.2018.07.031.
García-García, J., Ruiz-Romera, E., Martínez-Santos, M., Antigüedad, I., 2019. Temporal variability of metallic properties during flood events in the Deba River urban catchment (Basque Country, Northern Spain) after the introduction of sewage treatment systems. Environ. Earth Sci. 78, 23. https://doi.org/10.1007/s12665-018-8014-1.
Heaton, T.J., Köhler, P., Butzin, M., Bard, E., Reimer, R.W., Austin, W.E.N., Bronk Ramsey, C., Grootes, P.M., Hughen, K.A., Kromer, B., Reimer, P.J., Adkins, J., Burke, A., Cook, M.S., Olsen, J., Skinner, L.C., 2020. Marine20-the marine radiocarbon age calibration curve (0-55,000 cal BP). Radiocarbon 1–42. https://doi.org/10.1017/RDC.2020.68.
Ho, H.H., Swennen, R., Cappuyns, V., Vassilieva, E., Tran, T.V., 2012. Necessity of normalization to aluminium to assess the contamination by heavy metals and arsenic in sediments near Haiphong Harbor, Vietnam. J. Asian Earth Sci. 56, 229–239. https://doi.org/10.1016/j.jseaes.2012.05.015.
Horne, G.S., Patton, P.C., 1989. Bedload-sediment transport through the Connecticut River estuary. Geol. Soc. Am. Bull. 101, 805–819. https://doi.org/10.1130/0016-7606(1989)101<0805:BSTTTC>2.3.CO;2.
Horowitz, A.J., 1985. A Primer on Trace Metal-Sediment Chemistry. U.S. Geological Survey Water-Supply Paper 2277 (67 pp).
IHOBE, 1998. Investigación del suelo en la Comunidad Autónoma del País Vasco: Valores indicativos de evaluación (VIE-A, VIE-B, VIE-C) (116 pp.).
Irabien, M.J., Cearreta, A., Serrano, H., Villasante-Marcos, V., 2018. Environmental regeneration processes in the Anthropocene: the Bilbao estuary case (northern Spain). Mar. Pollut. Bull. 135, 977–987. https://doi.org/10.1016/j.marpolbul.2018.08.022.
Irabien, M.J., Cearreta, A., Gómez-Arozamena, J., Gardoki, J., Fernández Martín-Consuegra, A., 2020a. Recent coastal anthropogenic impact recorded in the Basque mud patch (southern Bay of Biscay shelf). Quat. Int. https://doi.org/10.1016/j.quaint.2020.03.042.
Irabien, M.J., Cearreta, A., Gómez-Arozamena, J., Gardoki, J., García-Artola, A., 2020b. Holocene vs Anthropocene sedimentary records in a human-altered estuary: the Pasaia case (northern Spain). Mar. Geol. 429, 106292. https://doi.org/10.1016/j.margeo.2020.106292.
Jayaraju, N., Sundara Raja Reddy, B.C., Reddy, K.R., 2010. Impact of dredging on sediment of Krishnapatnam Port, East Coast of India: implications for marine biodiversity. J. Environ. Sci. Eng. 4, 66–75.
Krishnaswamy, S., Lal, D., Martin, J.M., Meybeck, M., 1971. Geochronology of Lake sediment. Earth Planet. Sc. Lett. 11, 407–414. https://doi.org/10.1016/0012-821X(71)90202-0.
Lechuga-Crespo, J.L., Ruiz-Romera, E., Probst, J.L., Unda-Calvo, J., Cuervo-Fuentes, Z., Sánchez-Pérez, J.M., 2020. Combining punctual and high frequency data for the spatiotemporal assessment of main geochemical processes and dissolved exports in an urban river catchment. Sci. Total Environ. 727, 138644. https://doi.org/10.1016/j.scitotenv.2020.138644.
Legorburu, I., Rodríguez, J.G., Borja, A., Menchaca, I., Solaun, O., Valencia, V., Galparsoro, I., Larreta, J., 2013. Source characterization and spatio-temporal evolution of the metal pollution in the sediments of the Basque estuaries (Bay of Biscay). Mar. Pollut. Bull. 66, 25–38. https://doi.org/10.1016/j.marpolbul.2012.11.016.
Legorburu, L., Ramos, A., Sola, M., 1989. Heavy metals in coastal sediments in Guipuzcoa (Spain). Toxicol. Environ. Chem. 23, 129–134. https://doi.org/10.1080/02772248909357458.
Leorri, E., Cearreta, A., Irabien, M.J., Yusta, I., 2008. Geochemical and microfaunal proxies to assess environmental quality conditions during the recovery process of a heavily polluted estuary: the Bilbao estuary case (N. Spain). Sci. Total Environ. 396, 12–27. https://doi.org/10.1016/j.scitotenv.2008.02.009.
Loeblich, A.R., Tappan, H., 1988. Foraminiferal Genera and their Classification. Van Nostrand Reinhold, New York.
Lotze, H.K., Lenihan, H.S., Bourque, B.J., Bradbury, R.H., Cooke, R.G., Kay, M.C., Kidwell, S.M., Kirby, M.X., Peterson, C.H., Jackson, J.B.C., 2006. Depletion, degradation, and recovery potential of estuaries and coastal seas. Science 312, 1806–1809. https://doi.org/10.1126/science.1128035.
Martínez-Santos, M.M., Probst, A., García, J.G., Romera, E.R., 2015. Influence of anthropogenic inputs and a high-magnitude flood event on metal contamination pattern in surface bottom sediments from the Deba River urban catchment. Sci. Total Environ. 514, 10–25. https://doi.org/10.1016/j.scitotenv.2015.01.078.
Mojtahid, M., Geslin, E., Coynel, A., Gorse, L., Vella, C., Davranche, A., Zozzolo, L., Blanchet, L., Bénéteau, E., Maillet, G., 2016. Spatial distribution of living (Rose Bengal stained) benthic foraminifera in the Loire estuary (western France). J. Sea Res. 118, 1–16. https://doi.org/10.1016/j.seares.2016.02.003.
Montero, N., Belzunce-Segarra, M.J., Gonzalez, J.L., Larreta, J., Franco, J., 2012. Evaluation of diffusive gradients in thin-films (DGTs) as a monitoring tool for the assessment of the chemical status of transitional waters within the Water Framework Directive. Mar. Pollut. Bull. 64, 31–39. https://doi.org/10.1016/j.marpolbul.2011.10.028.
Murray, J.W., 2006. Ecology and Applications of Benthic Foraminifera. Cambridge University Press, Cambridge.
Nayar, S., Goh, B.P.L., Chou, L.M., Reddy, S., 2003. In situ microcosms to study the impact of heavy metals resuspended by dredging on periphyton in a tropical estuary. Aquat. Toxicol. 64, 293–306. https://doi.org/10.1016/S0166-445X(03)00062-6.
Newell, R.C., Seiderer, L.J., Hitchcock, D.R., 1998. The impact of dredging works in coastal waters: a review of the sensitivity to disturbance and subsequent recovery of biological resources on the sea bed. In: Ansell, A.D., Gibson, R.N., Barnes, M. (Eds.), Oceanography and Marine Biology: An Annual Review. CRC Press, Boca Raton, pp. 127–178.
Oldfield, F., 2014. Can the magnetic signatures from inorganic fly ash be used to mark the onset of the Anthropocene? Anthropocene Rev. 2, 3–13. https://doi.org/10.1177/2053019614534402.
Peñalver, X., San Jose, S., Mujika-Alustiza, J.A., 2017. El yacimiento arqueológico de Praileaitz I (Deba, Gipuzkoa, Euskal Herria). Metodología de la excavación, estratigrafía, estructuras y dataciones arqueológicas. In: Peñalver, X., San Jose, S., Mujika-Alustiza, J.A. (Eds.), La cueva de Praileaitz I (Deba, Gipuzkoa, Euskal Herria) Intervención arqueológica 2000–2009, Munibe Monographs: Anthropology and Archaeology Series, vol. 1, pp. 33–120.
Pérez, L., Borja, A., Rodríguez, G., Muxika, I., 2009. Long-term environmental, anthropogenic and climatic factors explaining spatial and temporal distribution of soft-bottom benthic communities within the Basque estuaries. Rev. Investig. Mar. 14, 1–22.
Perillo, G.M.E., 1995. Geomorphology and sedimentology of estuaries: an introduction. In: Perillo, G.M.E. (Ed.), Geomorphology and Sedimentology of Estuaries, Elsevier Developments in Sedimentology, vol. 53, pp. 1–16. https://doi.org/10.1016/S0070-4571(05)80021-4.
Prego, R., Boi, P., Cobelo-García, A., 2008. The contribution of total suspended solids to the Bay of Biscay by Cantabrian Rivers (northern coast of the Iberian Peninsula). J. Mar. Syst. 72, 342–349. https://doi.org/10.1016/j.jmarsys.2007.01.011.
Reimer, P., Austin, W., Bard, E., Bayliss, A., Blackwell, P., Bronk Ramsey, C., Butzin, M., Cheng, H., Edwards, R.L., Friedrich, M., Grootes, P.M., Guilderson, T.P., Hajdas, I., Heaton, T.J., Hogg, A.G., Hughen, K.A., Kromer, B., Manning, S.W., Muscheler, R., Palmer, J.G., Pearson, C., van der Plicht, J., Reimer, R.W., Richards, D.A., Scott, E. M., Southon, J.R., Turney, C.S.M., Wacker, L., Adolphi, F., Büntgen, U., Capano, M., Fahrni, S.M., Fogtmann-Schulz, A., Friedrich, R., Köhler, P., Kudsk, S., Miyake, F., Olsen, J., Reinig, F., Sakamoto, M., Sookdeo, A., Talamo, S., 2020. The IntCal20 northern hemisphere radiocarbon age calibration curve (0–55 cal kBP). Radiocarbon 1–33. https://doi.org/10.1017/RDC.2020.41.
Remondo, J., González-Díez, A., Díaz De Terán, J.R., Cendrero, A., 2003. Landslide susceptibility models Utilising spatial data analysis techniques. A case study from the lower Deba Valley, Guipúzcoa (Spain). Nat. Hazards 30, 267–279. https://doi.org/10.1023/B:NHAZ.0000007202.12543.3a.
Rivas, V., Cendrero, A., 1992. Análisis histórico de la evolución superficial de los estuarios del País Vasco. Lurralde 15, 199–227.
Rivas, V., Remondo, J., Bonachea, J., Sánchez-Espeso, J., 2021. Rainfall and weather conditions inducing intense landslide activity in northern Spain (Deba, Guipúzcoa). Nat. Hazards Earth Syst. Sci. https://doi.org/10.5194/nhess-2019-416 (in press).
Robbins, J.A., 1978. Geochemical and geophysical applications of radioactive lead. In: Nriagu, J.O. (Ed.), The Biogeochemistry of Lead in the Environment, Part A. Elsevier, Amsterdam, pp. 285–293.
Rodríguez, R.G., Tueros, I., Borja, A., Belzunce, M.J., Franco, J., Solaun, O., Valencia, V., Zuazo, A., 2006. Maximum likelihood mixture estimation to determine metal background values in estuarine and coastal sediments within the European Water Framework Directive. Sci. Total Environ. 370, 278–293. https://doi.org/10.1016/j.scitotenv.2006.08.035.
Rose, N.L., 2015. Spheroidal carbonaceous fly ash particles provide a globally synchronous stratigraphic marker for the Anthropocene. Environ. Sci. Technol. 49, 4155–4162. https://doi.org/10.1021/acs.est.5b00543.
Ruiz, F., González-Regalado, M.L., Borrego, J., Abad, M., Pendón, J.G., 2004. Ostracoda and foraminifera as short-term tracers of environmental changes in very polluted areas: the Odiel Estuary (SW Spain). Environ. Pollut. 129, 49–61. https://doi.org/10.1016/j.envpol.2003.09.024.
Ruiz-Fernández, A.C., Sanchez-Cabeza, J.A., Serrato de la Peña, J.L., Pérez Bernal, L.H., Cearreta, A., Flores-Verdugo, F., Machain, M., Chamizo, E., García-Tenirio, R., Queralt, I., Dunbar, R., Mucciarone, D., Diaz Asencio, M., 2016. Accretion rates in coastal wetlands of the southeastern Gulf of California and their relationship with

sea-level rise. Holocene 26, 1126–1137. https://doi.org/10.1177/0959683616632882.
Samir, A.M., El-Din, A.B., 2001. Benthic foraminiferal assemblages and morphological abnormalities as pollution proxies in two Egyptian bays. Mar. Micropaleontol. 41, 193–227. https://doi.org/10.1016/S0377-8398(00)00061-X.
Sanchez-Cabeza, J.A., Ruiz-Fernández, A.C., 2012. ^{210}Pb sediment radiochronology: an integrated formulation and classification of dating models. Geochim. Cosmochim. Ac. 82, 183–200. https://doi.org/10.1016/j.gca.2010.12.024.
Santschi, P.H., Presley, B.J., Wade, T.L., García-Romero, B., Baskaran, M., 2001. Historical contamination of PAHs, PCBs, DDTs, and heavy metals in Mississippi River Delta, Galveston Bay and Tampa Bay sediment cores. Mar. Environ. Res. 52, 51–79. https://doi.org/10.1016/S0141-1136(00)00260-9.
Solaun, O., Rodríguez, J.G., Borja, A., Larreta, J., Valencia, V., 2015. Relationships between polychlorinated biphenyls in molluscs, hydrological characteristics and human pressures, within Basque estuaries (northern Spain). Chemosphere 118, 130–135. https://doi.org/10.1016/j.chemosphere.2014.07.053.
Soulsby, R.L., Mead, C.T., Wild, R., Wood, M.J., 2007. A model for simulating the dispersal tracks of sand grains in coastal areas: “SandTrack”. Geol. Soc. Spec. Publ. 274, 65–72. https://doi.org/10.1144/GSL.SP.2007.274.01.08.
Sreenivasulu, G., Jayaraju, N., Sundara Raja Reedy, B.C., Lakshmi Prasad, T., Nagalakshmi, K., Lakhsmanna, B., 2017. Foraminiferal research in coastal ecosystems in India during the past decade: a review. Geo. Res. J. 13, 38–48. https://doi.org/10.1016/j.grj.2017.02.003.
Sun, J., Wang, M.H., Ho, Y.S., 2012. A historical review and bibliometric analysis of research on estuary pollution. Mar. Pollut. Bull. 64, 13–21. https://doi.org/10.1016/j.marpolbul.2011.10.034.
Swindles, G.T., Watson, E., Turner, T.E., Galloway, J.M., Hadlari, T., Wheeler, J., Bacon, K.L., 2015. Spheroidal carbonaceous particles are a defining stratigraphic marker for the Anthropocene. Sci. Rep. 5, 10264. https://doi.org/10.1038/srep10264.
Takata, H., Tanaka, S., Seto, K., Sakai, S., Takayasu, K., Khim, B.K., 2014. Biotic response of benthic foraminifera in Aso-Kai lagoon, Central Japan, to changes in terrestrial climate and ocean conditions (~AD 700–1600). J. Paleolimnol. 51, 421–435. https://doi.org/10.1007/s10933-014-9764-8.
Tueros, I., Rodríguez, J.G., Borja, A., Solaun, O., Valencia, V., Millán, E., 2008. Dissolved metal background levels in marine waters, for the assessment of the physicochemical status, within the European Water Framework Directive. Sci. Total Environ. 407, 40–52. https://doi.org/10.1016/j.scitotenv.2008.08.026.
Tueros, I., Borja, A., Larreta, J., Rodríguez, J.G., Valencia, V., Millán, E., 2009. Integrating long-term water and sediment pollution data, in assessing chemical status within the European Water Framework Directive. Mar. Pollut. Bull. 58, 1389–1400. https://doi.org/10.1016/j.marpolbul.2009.04.014.
Valencia, V., Franco, J., Borja, A., Fontán, A., 2004. Hydrography of the southeastern Bay of Biscay. In: Borja, A., Collins, M. (Eds.), Oceanography and Marine Environment of the Basque Country, Elsevier Oceanography Series, vol. 70, pp. 159–194. https://doi.org/10.1016/S0422-9894(04)80045-X.
Van Cauwenberghe, L., Devriese, L., Galgani, F., Robbens, J., Janssen, C.R., 2015. Microplastics in sediments: a review of techniques, occurrence and effects. Mar. Environ. Res. 111, 5–17. https://doi.org/10.1016/j.marenvres.2015.06.007.
Villate, F., Franco, J., Ruiz, A., Orive, E., 1989. Caracterización geomorfológica e hidrológica de cinco sistemas estuáricos del País Vasco. Kobie (Serie Ciencias Naturales) 18, 157–170.
Walker, M., Head, M.J., Lowe, J., Berkelhammer, M., Björck, S., Cheng, H., Cwynar, L.C., Fisher, D., Gkinis, V., Long, A., Newnham, R., Rasmussen, S.O., Weiss, H., 2019. Subdividing the Holocene Series/Epoch: formalization of stages/ages and subseries/subepochs, and designation of GSSPs and auxiliary stratotypes. J. Quat. Sci. 34, 173–186. https://doi.org/10.1002/jqs.3097.
Walton, W.R., 1952. Techniques for recognition of living foraminifera. Cont. Cushman Found. Foram. Res. 3, 56–60.
Wang, J., Zhang, W., Baskaran, M., Du, J., Zhou, F., Wu, H., 2018. Fingerprinting sediment transport in river-dominated margins using combined mineral magnetic and radionuclide methods. J. Geophys. Res. Oceans 123, 5360–5374. https://doi.org/10.1029/2018JC014174.
Wang, P., Murray, J.W., 1983. The use of foraminifera as indicators of tidal effects in estuarine deposits. Mar. Geol. 51, 239–250. https://doi.org/10.1016/0025-3227(83)90106-8.
Zalasiewicz, J., Waters, C.N., Williams, M., Barnosky, A.D., Cearreta, A., Crutzen, P., Ellis, E., Ellis, M.A., Fairchild, I.J., Grinevald, J., Haff, P.K., Hajdas, I., Leinfelder, R., McNeill, J.R., Odada, E., Poirier, C., Richter, D., Steffen, W., Summerhayes, C., Syvitski, J., Vidas, D., Wagreich, M., Wing, S.L., Wolfe, A.P., Zhisheng, A., Oreskes, N., 2015. When did the Anthropocene begin? A mid-twentieth century boundary level is stratigraphically optimal. Quat. Int. 383, 196–203. https://doi.org/10.1016/j.quaint.2014.11.045.